The mandible and dentition of Borealestes serendipitus (Docodonta) from the Middle Jurassic of Skye, Scotland

The mandible and dentition of *Borealestes serendipitus* (Docodonta) from the Middle Jurassic of Skye, Scotland

Journal:	*Journal of Vertebrate Paleontology*
Manuscript ID	JVP-2018-0110.R2
Manuscript Type:	Article
Date Submitted by the Author:	n/a
Complete List of Authors:	Panciroli, Elsa; National Museum of Scotland, ; University of Edinburgh School of GeoSciences Benson, Roger; University of Oxford, Department of Earth Sciences Luo, Zhe-Xi; The University of Chicago, Department of Organismal Biology & Anatomy
Key Words:	Borealestes, Mammaliaformes, Middle Jurassic, Scotland, Docodonta

The mandible and dentition of *Borealestes serendipitus* (Docodonta) from the Middle Jurassic of Skye, Scotland

ELSA PANCIROLI,[1,2]* ROGER B.J. BENSON,[3] and ZHE-XI LUO[4]*

[1] Natural Science Department, National Museums Scotland, Edinburgh, Scotland, EH1 1JF, United Kingdom;

[2] School of Geosciences, Grant Institute, University of Edinburgh, Scotland, EH9 3JW, United Kingdom, *elsa.panciroli@ed.ac.uk;

[3] Department of Earth Sciences, University of Oxford, Oxford, England, United Kingdom. roger.benson@earth.ox.ac.uk;

[4] Department of Organismal Biology and Anatomy, The University of Chicago, Chicago, Illinois, U.S.A. zxluo@uchicago.edu

* Corresponding author

ABSTRACT—The Middle Jurassic docodont *Borealestes serendipitus* was the first Mesozoic mammal found in Scotland over forty years ago. Its affinities and morphology remain poorly understood. Although multiple dentary fragments and isolated teeth have been recovered from Scotland and England, they have not yet been described in sufficient detail. We report new, more complete specimens collected during recent field work on Skye, Scotland, combined with previously collected material. This includes upper and lower dentition and an almost complete right dentary. We present an updated description and diagnosis of the genus *Borealestes*, based on high resolution micro-CT and synchrotron scans. We identify seven key features that distinguish *Borealestes* from other docodonts, including a pronounced a–c crest, absence of the a–g crest on cusp a, an anterior fovea at the buccolingual midpoint of the upper molar, and the convergence of the Meckel's groove with the ventral margin of the mandible. We also present a revised diagnosis for the second species, *B. mussettae*. Our phylogenetic analysis supports a clade formed by *Borealestes*, *Haldanodon*, *Docofossor* and *Docodon*. Ontogenetic variation in the mandibular morphology of *Borealestes* is similar to that seen in *Docodon* and *Haldanodon*, with the delayed emergence of the ultimate lower molar, the shift of the last molar to the front of the coronoid process, and a posterior shift of the Meckel's sulcus in successively older individuals. This supports a distinctive growth pattern in the clade including *Borealestes* and *Docodon*, one that may be present in Docodonta as a whole.

INTRODUCTION

Docodonta are an extinct clade of mammaliaforms that fall outside the mammalian crown group, and are therefore important for understanding the morphological evolution of mammals as a whole (Simpson, 1929; Lillegraven and Krusat, 1991). Docodonts were previously thought to be closely related to Morganucodonta due to some shared features (Hopson and Crompton, 1969; Kermack et al., 1973), or as the basal-most clade of stem mammals (= Mammaliaformes) (Lillegraven and Krusat, 1991). However, in recent decades more complete cranial and skeletal material has led to the consensus that the Docodonta clade is closer to crown group mammals than to *Sinoconodon* and Morganucodonta (Wible and Hopson, 1993; Luo, 1994; Luo et al., 2002; Martin, 2005). In some recent phylogenetic assessments of stem mammaliaforms, docodonts are more basal than Kuehneotheria (Gill, 2004) and haramiyidans (e.g., Luo et al., 2015a; 2017). It has been suggested that docodonts are more closely related to Late Triassic mammaliaforms such as *Tikitherium*, *Woutersia,* and *Delsatia*, but these hypothesized relationships are currently based on the isolated molars of these taxa, and are tentative at the best (Sigogneau-Russell and Hahn, 1995; Datta, 2005; Luo and Martin, 2007; Averianov et al., 2010).

All docodonts share a highly distinctive dental morphology, and they were one of the first mammaliaform clades to emerge across Eurasia in the Middle Jurassic (Lopatin and Averianov, 2005; Waldman and Savage, 1972; Luo and Martin, 2007). They are particularly abundant in fossil deposits of the Middle–

Late Jurassic (Hu et al., 2006; Luo, 2007; Averianov et al., 2010; Martin et al., 2010; Meng et al., 2015; Rougier et al., 2015).

The postdentary elements—homologs to mammalian middle ear—remain attached to the dentary in docodonts, a plesiomorphic characteristic in stem mammaliaforms (Lillegraven and Krusat, 1991; Ji et al., 2006; Luo, 2011; Meng et al., 2015). Nevertheless, docodonts are unique among Mesozoic clades in possessing distinctively complex molar cusps and crests. It is generally accepted that docodont molars are capable of versatile shearing and crushing functions not seen in other stem group mammaliaforms (Jenkins, 1969; Gingerich, 1973; Butler, 1997; Schultz et al., 2017). This may have contributed to their unusually diverse ecological specialisations. Docodonts are now known to have had very divergent locomotor morphologies, including semi-aquatic, fossorial, and arboreal specialisations, as revealed by well-preserved postcranial skeletons (Ji et al.,2006; Luo et al., 2015b; Meng et al., 2015).

Borealestes from the UK (Waldman and Savage, 1972; Sigogneau-Russell, 2003) is among the geologically oldest docodonts, being Bathonian in age. *Castorocauda* and *Agilodocodon* from China are also possibly from the latest Bathonian (Meng et al., 2015; Xu et al., 2017). The youngest record for Docodonta is *Sibirotherium* from the Early Cretaceous of Russia (Maschenko et al., 2002). Docodonta were most diverse in the Middle Jurassic, and had a Laurasian distribution—this is with the possible exception of *Gondtherium* from Toarcian sediments in India (Prasad and Manhas, 2001, 2007). However, due to a paucity of material and poor preservation, the docodont affinities of

Gondtherium are currently unresolved (Kielan-Jawarowska et al., 2004; Averianov et al., 2010).

The holotype of *Borealestes serendipitus* was discovered in the Kilmaluag Formation (Bathonian) of the Isle of Skye in the 1970s, and was the first Mesozoic mammal to be found in Scotland (Waldman and Savage, 1972). The holotype comprises a fragment of dentary, and three other dentary fragments were reported at the same time and referred to *B. serendipitus* by preliminary identification. These additional specimens are described here for the first time. A partial mammal skeleton of uncertain affinity was also collected from Kilmalaug Formation in early 1970s. We can now confirm the identity of this specimen as *Borealestes serendipitus* herein, on the basis of its almost complete dentary, along with associated upper molars, and incisors. The characteristics of these parts of the fossil are described here (the rest of the skeleton is currently under study by EP; Panciroli et al., 2018).

Isolated molars of *B. serendipitus* were later recovered from the Forest Marble Formation in Kirtlington (Sigogneau-Russell, 2003) and Watton Cliff (Evans, 1992) in England, all Bathonian (Middle Jurassic) in age. A second species, *B. mussettae*, was later erected based on molars from Kirtlington (Sigogneau-Russell, 2003). Multiple specimens from Kirtlington have been referred to *B. serendipitus* and *B. mussettae*, but not all specimens have been fully described.

Additional specimens of *Borealestes serendipitus* have been recovered during recent field work on the Isle of Skye, along with several other Mesozoic

mammaliaforms including the cladotherian mammal *Palaeoxondon ooliticus*, and the morganucodontan *Wareolestes rex* (Close et al., 2016; Panciroli et al., 2017a, 2018b). Material found during field work in 2016 includes another dentary of *Borealestes* (NMS G.2018.27.1, found by EP).

We re-examine previously collected material and combine it with newly collected specimens. We provide a full description of the dental and mandibular morphology of *Borealestes serendipitus*. This includes: the complete lower dentition and dental formula; postdentary trough and its related structures; Meckel's groove; efflected angular process; dentary peduncle; and nerve and blood vessel channels within the dentary. Based on this body of new information we provide a revised and expanded diagnosis for the genus *Borealestes*, and distinguishing features of *B. serendipitus* and *B. mussettae*. We have also reviewed the material for *Borealestes* in light of this diagnosis, and updated the referred specimen lists accordingly. We find evidence for ontogenetic changes in mandibular structures, as recently described in *Docodon* (Schultz et al., 2017). The more complete documentation of the dental and mandibular morphology of *Borealestes* provides new characters for an updated phylogenetic analysis of all docodonts including *Borealestes*.

GEOLOGICAL BACKGROUND

The Kilmaluag Formation on the Isle of Skye crops out on the Scottish Inner Hebridean Islands of Eigg, Skye and Muck. It was formerly known as the

Ostracod Limestone, as the base of the formation is defined by the occurrence of ostracod-bearing calcareous and fissile mudstones (Barron et al., 2012). Although exact biostratigraphical correlations with Jurassic sites in England have proven difficult, the Kilmaluag Formation is now considered to be late Bathonian in age, and to correlate with the Forest Marble Formation at Kirtlington Cement Quarry in Oxfordshire (Barron et al., 2012). The similarities in vertebrate faunal composition with Kirtlington Cement Quarry also supports a late Bathonian age for these localities.

Unlike other formations within the Great Estuarine Group, the Kilmaluag Formation includes predominantly freshwater facies, and there are abundant freshwater ostracods such as *Darwinula* (Wakefield, 1995), shallow freshwater to oligohaline conchostracans (Chen and Hudson, 1991) and freshwater gastropods (Andrews, 1985; Morton and Hudson, 1995; Barron et al., 2012). Paleoenvironmental reconstructions suggest a low-salinity environment of closed off lagoons with freshwater input, occasionally drying out to form mudcracks (Andrews, 1985). Highly fossiliferous vertebrate-bearing beds of the Kilmaluag Formation are located on the Strathaird Peninsula and comprise micritic grey limestones with detrital quartz and clay in varying fractions. Vertebrate remains include fish and sharks, turtles, crocodilomorphs, pterosaurs, lepidosaurs, choristoderes, mammaliaforms and tritylodontids, as well as some dinosaur fossils (Waldman and Savage, 1972; Evans et al., 2005; Barrett, 2006; Anquetin et al., 2009, 2010; Wills et al., 2014; Close et al., 2016; Panciroli et al., 2017a, 2017b, 2018).

The mammal bed at Kirtlington Cement Quarry in Oxfordshire, England, yields fossils from the Forest Marble Formation. It is late Bathonian in age, and is the most productive microvertebrate site of the Middle Jurassic in the UK. The Mammal Bed comprises unconsolidated marly clay overlying a coral limestone, with freshwater gastropods and ostracods suggesting a marginal coastal habitat (Evans and Milner, 1994; Barron et al., 2012). The assemblage there includes similar taxa to the Kilmaluag Formation: amphibian, lepidosaur, archosaur, choristodere, dinosaur and fish remains, as well as mammal species and a tritylodontid, which are represented by individual teeth, jaw fragments, and some cranial and postcranial elements (Freeman, 1979; Kermack, 1988; Evans and Milner, 1994).

Watton Cliff, also known as Westcliff, is a late Bathonian site in Dorset, England, that is also part of the Forest Marble Formation. It comprises ~26 meters of argillaceous sediments, divided in half by hard, shelly limestone calcirudites (Holloway, 1983; Evans, 1992). It is considered to be a higher energy sedimentary environment, likely an offshore shell bank, with channels cut by storms and filled with terrestrial debris (Holloway, 1983; Barron et al., 2012). It has yielded tritylodontid, amphibian, shark, teleosauroid, and small archosaur fossils, mostly teeth (Evans, 1992; Evans and Milner, 1994).

MATERIALS AND METHODS

Most of the micro-computed tomographic data (microCT) were obtained at the University of Bristol using a Nikon XTH225ST scanner with a 225kV rotating target with a peak energy of 140 kV. Resolution varies between specimens: BRSUG 20570, BRSUG20571, BRSUG29007and NMS G.1992.47.121.4 are 6.77 µm; and NMS G.1992.47.121.3 is 12.77µm. Synchrotron data for NMS G.2018.27.1 and NMS G.1992.47.121.1 were obtained at the European Synchrotron Radiation facility (ESRF), Grenoble, France. The resolution for NMS G.2018.27.1 is 6.35 µm. For NMS G.1992.47.121.1 the scan resolution was 6.15 µm, which was subsequently resampled to 12.3 µm. All microCT and synchrotron scans were digitally reconstructed and image processed using Mimics 19.0 at the National Museum of Scotland, Edinburgh. Specimens were also observed using conventional microscopy. All digital reconstructions can be found in the online depository: www.morphosource.org

Measurements were taken from digitally reconstructed microCT scans in Mimics 19.0. It is unclear in previous studies how molar measurements were taken, so in order to standardise our measurements, we measured as follows (Fig. 1): for lower molar length we measured across the length of the tooth anteroposteriorly from cusps d to b, and cusps df to e; for upper molar length we measured the longest length on the labial part of the molar, and the longest on the lingual wing of the molar. For lower molar width we measured mediolaterally across cusp c, and across cusp g at right angles (in occlusal view) to the length measurement from cusp d to cusp b. For width of upper molars we measured across cusp X to midway anteroposteriorly along the buccal edge of the molar.

Premolar and canine tooth measurements were taken anteroposteriorly from most anterior to most posterior edge of the crown, and mediolateral width was taken across the cusp of the tooth at the base of the crown. Although the latter width was not always the widest due to slight bulging of the cingulid in the premolars, measuring in this way provides a more consistent measurement and the difference was usually ≤ 0.1 mm.

We analysed the character matrix used by Meng et al. (2015) including updated and rescored character states for *Borealestes serendipitus* and *Borealestes mussettae*. This data matrix has 23 taxa (24 with *B. mussettae*) scored for 48 characters of the dentary (47 in the original matrix, with one additional character), and upper and lower dentition. Of these taxa, fourteen are docodonts and nine are other mammaliaforms, including *Gondtherium*, a disputed docodont (Averianov et al., 2010), which is now found to fall outside of Docodonta (Meng et al., 2015).

Some character states for the other taxa in the matrices provided in Meng et al. (2015) differed between the character listing, NEXUS and PAUP sections of their supplementary materials. Therefore, we re-assessed all of these character states for this analysis (see Supplementary material for complete character list, character matrix, and details of updated and rescored characters).

We analysed these data as for Meng et al. (2015), using PAUP* 4.0. A branch and bound tree search was conducted using parsimony with characters unordered and equally-weighted. One tree of 117 steps was retained. Our time-scaled phylogeny was created in R using the strap package. First and last

appearance data (FADLAD) were taken from fossilworks.org, except for *Borealestes* species, where stratigraphic dates of formations were used from Holloway (1983) and Barron et al. (2012). The stratigraphic ages of the Chinese docodonts *Docofossor*, *Castorocauda* and *Agilodocondon* were adopted from Xu et al. (2017).

Institutional Abbreviations—**BRSUG**, Geology Museum, University of Bristol, UK (formerly UBGM); **NHMUK**, Natural History Museum, London, UK; **NMS**, National Museum of Scotland, Edinburgh, UK (formerly RMS); **OUMNH**, Oxford University Museum of natural History.

Terminology—We follow Luo and Martin (2007) in the designation of cusps with letters, and using abbreviated crest designations according to their connections to cusps, combined with topographic descriptors to specify their locations on the tooth (Fig. 1). This nomenclature is based on a combination of alphabetical nomenclature from Butler (1997), and descriptive definitions from Sigogneau-Russell (2003), supplemented by Kielan-Jaworowska et al. (2004) and Pfretzschner et al. (2005). In addition, we provide a table of descriptive definitions as used by previous authors (Supplementary Table 1). We preferentially use ‘buccal’ throughout the descriptive text, but retain the use of ‘labial’ for some terminology to provide ease of comparison with previous publications.

SYSTEMATIC PALEONTOLOGY

MAMMALIAFORMES Rowe, 1988 (emended)

DOCODONTA Kretzoi, 1946

DOCODONTIDAE Simpson, 1929

BOREALESTES Waldman and Savage, 1972

Revised Diagnosis—Dental formula 4.1.?5.4/ 4.1.5.6. Upper molars of *Borealestes*: buccolingually wide and mesiodistally short; upper molars 'figure 8' shape, with anteroposteriorly constricted waist; two main buccal cusps, A and C, plus a small cusp B in the buccomesial corner; lingual half of the upper molar has main anterior lingual cusp X; cusp X larger and more prominent than smaller posterior lingual cusp Y; labial cusps connected by a ridge/ridges anteroposteriorly; transverse ridge extends between the main anterior labial cusp A and the main lingual cusp X. Lower molars: elongated anteroposteriorly, with labial row of higher cusps arranged in anterioposterior alignment with largest cusp a, and lingual row of smaller cusps with distinctive anterior cusp g and larger posterior cusp c; lower molars have cusps b–a–c in a triangular arrangement. Docodonts differs from other mammaliaforms but similar to pseudotribosphenids in possessing an anterior 'pseudotalonid basin'—anterior to the 'trigonid'—formed by cusps a, b and g. Docodonts possess the plesiomorphic mammaliaform trait of attachment of postdentary elements to the dentary. *Borealestes* has an efflected angular process (sensu Simpson, 1929) and an enlarged medial ridge protuberance (sensu Schultz et al., 2017), both are docodont autapomorphies. *Borealestes* possesses enlarged and pointed upper and lower canines that are two-rooted, as in other docodonts.

Among docodonts, *Borealestes* most closely resembles *Krusatodon, Castorocauda* and *Haldanodon* in lower molar morphology. These taxa share the derived feature of a larger cusp c than cusp g. It resembles *Castorocauda* and possibly also *Itatodon* in having a slightly recurved cusp c. *Borealestes* possesses an anterior 'cingulid' on the lower molars incorporating cusp e, similar to *Castorocauda* and *Docodon*. Cusp e is anteriorly projecting and forms part of the d–df-e interlock with the neighbouring molar, as in *Krusatodon* and *Simpsonodon*. On the premolars *Borealestes* has a distinct lingual cingulid and a posterior labial cingulid, as seen in most other docodontans. Unlike *Simpsonodon, Agilodocodon*,and *Docodon*, but like most other docodonts, *Borealestes* does not have dense creases and pits or other ornamentation on molar enamel surfaces. *Borealestes* species have a very distinctive a–c crest.

In upper molar morphology, *Borealestes* differs from all other docodonts except *Docodon* in having an anterior fovea: a concave area anterior to the anterolingual crest. *Borealestes* differs from *Docodon* in having the anterior fovea positioned at the anteroposteriorly constricted waist of the upper molars. *Borealestes* differs from *Krusatodon, Agilodocodon, Simpsonodon, Docodon* and *Haldanodon,* in having transversely expanded and anteroposteriorly slightly compressed lingual wing of the upper molar, which is similar to *Docofossor* and *Dsungarodon*. The posterior upper molars are similar to *Haldanodon*, *Docofossor*, to some extent also to *Docodon*. *Borealestes* resembles *Docofossor* and *Dsungarodon* in having more reduced cusps Y and Z on the upper molars, and a larger cusp X.

BOREALESTES SERENDIPITUS Waldman and Savage, 1972

Holotype—BRSUG 20570, fragment of left dentary from the Kilmaluag Formation, Isle of Skye.

Referred Specimens—BRSUG 20571 fragment of left dentary; BRSUG 29007 fragment of right dentary; BRSUG 29008 three fragmentary molars in matrix – all from the Kilmaluag Formation, Isle of Skye. NMS G.1992.47.121.1, partial skeleton that includes upper molar rows and some incisors; NMS G.1992.47.121.3, almost complete right dentary detached from NMS G.1992.47.121.1; NMS G.2018.27.1, fragment of right dentary in matrix; NMS G.1992.47.121.4 (previously BRSUG 29006) anterior upper incisors, premaxilla and nasal fragment – all from the Kilmaluag Formation, Isle of Skye.; OUMNH J.79474, OUMNH J.79475, and OUMNH 79498, all isolated lower molars - all from the Forest Marble Formation of Kirtlington, Oxfordshire. Lower molars NHMUK PV M46039, NHMUK PV M46521, NHMUK PV M46549, NHMUK PV M46610, NHMUK PV M46632, NHMUK PV M46728, NHMUK PV M46791, NHMUK PV M46841, NHMUK PV M46842, NHMUK PV M46845, NHMUK PV M46869, NHMUK PV M46389, NHMUK PV M46399, NHMUK PV M46401, NHMUK PV M46588, and upper molars NHMUK PV M46316, NHMUK PV M46396, and possibly NHMUK PV M46607 (uncertain) - all from the Forest Marble Formation of Kirtlington, Oxfordshire. NHMUK PV M46058, NHMUK PV M44301 and probably NHMUK PV M46116, all lower molars from the Forest Marble Formation of Watton Cliff, Dorset. (The following specimens were referred

to *B.* serendipitus, but were re-identified during this study: OUMNH J.79446 re-identified as *Krusatodon* or *Simpsonodon*, OUMNH 79497 re-identified as *Simpsonodon*; OUMNH J.79514 re-identified as *Krusatodon*; NHMUK PV M46580 re-identified as *B. mussettae*; NHMUK PV M46445 possibly *Krusatodon*; NHMUK PV M46066 not *B. serendipitus*, but identification uncertain. See Supplementary Material for details).

Revised Diagnosis—*B. serendipitus* differs from all other docodonts and from *B. musetti* in that the primary cusp a has a rounded surface and as result an absence of the a–g crest on cusp a (present to variable extent on cusp g) and the absence of an a–d crest on cusp a (but a labially oriented a–d crest is present on cusp d). *B. serendipitus* has a stronger and more elevated b–g crest and c–d crest, than *B. mussettae*. Cusp e in *B. serendipitus* is positioned more lingually than in *B. mussettae*. *B. serendipitus* differs from *B. mussettae* in having a distinct anterolabial and anterolingual crest between cusps A and X in the upper molars, and in that cusp Z is reduced. The anterior fovea is more distinct than in *B. mussettae*.

DESCRIPTION

Upper Tooth Row

NMS G.1992.47.121.4 is a rostral skull fragment consisting of the premaxillae and a part of one nasal of *Borealestes serendipitus*. This component belongs to the same partial skeleton as the upper molars (below), NMS

G.1992.47.121.1 (currently under study by EP). This skull component became separated from the rest of the skeleton in the 1980s, after collection of this fossil in the field in the early 1970s. It was accessioned to the University of Bristol (as BRSUG 29006), but was subsequently relocated to National Museums Scotland where the rest of the skeleton is held.

The premaxilla of NMS G.1992.47.121.4 has the right I1 and I2 and a partial root of I3, the left I2 root, and the complete left I3 and I4 (Fig. 2). Combining the information from the right and the left incisors, we determine that *B. serendipitus* possesses four upper incisors. It has a single-rooted I1 with a leaf shaped crown, which has a convex external (buccal) surface and a concave internal (lingual) surface with a lingual cingulum (Fig. 2A1, C1–2). The roots of I2 to I4 are deeply bifurcated, diverging at their tips. This bifurcation is similar to that seen in *Agilodocodon* (Meng et al., 2015: fig. s2) and *Haldanodon* (Krusat, 1980). The crowns of I2 to I4 are caniniform in lateral outline: they are recurved, and the anterior edge of the tooth is convex and smooth. The buccal aspect of I2–I4 is gently convex and the lingual aspect is broadly concave with a ridge running from the apex of the crown to the base. There is a weak lingual cingulum with a small cuspule on the posteriormost edge, which connects to the incisor apex via a curved low ridge. This overall morphology of upper incisors of *Borealestes* is similar to *Agilodocodon.*

The upper molars and premolars preserved with the partial skeleton of *Borealestes serendipitus* NMS G.1992.47.121.1 include: roots of right P4 and P5, and almost complete M1 to M4 (Fig. 2A1); and the partial roots of left P5, and

almost complete M1 to M4 (Fig. 2A2) (for tooth measurements see Table 1). The premolar-molar boundary in *Borealestes* (as for docodonts as a whole) can be clearly defined as two roots for the ultimate premolars and three roots for the first molar, which we also observe here.

The molars are transversely wide and have a figure-of-eight shaped outline in occlusal view. This occurs due to the anteroposterior mid-point constriction of the molar, which creates a distinct lingual wing (Fig. 2A1–2). The lingual wing comprises a large cusp X, a smaller, more posterior cusp Y, and a much smaller cusp Z positioned on the anterior cingular margin of the tooth. The labial portions of the molar crown on right M1–3 and on left M1–3 are missing due to wear after exposure in the field. The buccodistal corner of M3 on both sides is preserved, and the M4s are well preserved. Although the left and right M3s are missing cusp A, the broad base of this cusp indicates that it is larger than cusp C, and both are positioned in anteroposterior alignment (Fig. 2A1–2). A transverse crest connects cusps A and X. This crest is nearly continuous and is made up of the anterolabial and anterolingual crests. The transverse crest leading from cusp Y is not distinct, and only extends to the midpoint constriction of the crown. This crest does not extend further buccally and has no connection to the rounded cusp C or the buccodistal cingulum.

M4 is reduced, especially mesiodistally, and as such it is smaller than M3. M4 has a much reduced cusp C. Cusps A and C are joined by a short A–C crest, and both cusps are more lingually positioned, than on the preceding molars.

We infer that in all upper molars, there is an anterior crest running from cusp A to the position of an indistinct 'cusp B', as best seen in the right M3 (Fig. 2A1). This feature is incomplete in some upper molars where this region is broken/abraded. The upper molars have a buccal cingulum, which takes the form of a thin line, rather than a fully formed crest. The buccal margin is indented by an ectoflexus. The buccal cingulum is also present in what remains of both M3.

There is a distinct occlusal basin at the point of mid constriction, formed between cusps C and Y, and posterior to A–X crest, on all upper molars. This is functionally analogous to the trigon basin of the tribosphenic upper molars. This is a general feature shared by most docodonts, with the exception of *Docofossor* (Luo et al., 2015b). There is a distinctly concave region anterior to the anterolabial and anterolingual crest (connecting cusps A–X), near the buccolingual mid-point of the crown. This is formed partly because of the mid-point constriction of the tooth and partly by the saddle-shape of the anterolabial and anterolingual crests. We have named this area the anterior fovea of the upper molars (Fig. 1B, 2, 7C–E). The anterior fovea is present in *Borealestes* and *Docodon*, but in *Docodon* the fovea is positioned more lingually on the anterior face of cusp X. We interpret the buccolingual midpoint position of the anterior fovea as a diagnostic feature of *Borealestes*.

A minor difference between M4 and more anterior molars is that the posterior half of M4 is more reduced such that the A–X crest almost becomes the transverse midline across the tooth crown (Fig. 2A1–2). The M4 crown bears

strong resemblance to the upper molars of *Haldanodon* by this placement of this crest, and by the mid-point constriction.

The molar crowns bulge outwards from the roots at their bases where they meet the alveolar margin (Fig. 2B1, C1). There are three roots per molar, and they are straight except for M4. The roots of M4 curve anteriorly, suggesting that during the eruption of this tooth, the tooth rotated, causing the bending of the roots. M4 roots are slightly shorter that the other molar roots. All of the upper molar roots widen towards their base in the maxillary alveolar margin. Roots of upper molars, especially the lingual root and posterior root, tend to have slightly inflated root-tips, indicating ontogenetic cessation of root growth.

Lower Tooth Row

The morphology of five dentaries including the holotype BRSUG 20570 confirm the diagnosis and morphology of *Borealestes serendipitus* (see Table 1 for tooth measurements). The holotype comprises part of the left dentary containing the posterior root of p3, intact p4 and p5, and fully erupted m1 to m4 (Fig. 3). Although the crown of m5 is lost, the roots are in place within the dentary, and a hidden (but almost erupted) m6 is present (Fig. 3). Only a thin wall of bone separates the anterior alveolus of m6 and the posterior alveolus of m5. There is sign of bone regrowth just below the rim of the m5 alveolus (Fig. 3F), suggesting possible (traumatic) pre-mortem loss of this molar. BRSUG 20571 is a fractured section of left dentary (Fig. 4A–E). It is broken anteriorly at the position of m1, and posteriorly behind the coronoid scar and depression that

represents the entrance of the mandibular nerve (V3 notch). The roots of m1, roots and base of the crown of m2, the almost complete crown of m3, most of m4, and almost complete m5 remain in the dentary. The ultimate molar (m5) is much reduced in crown size, and the two roots are fused along much of their length, typical of the ultimate lower molars of docodonts. Only m3 has a preserved cusp a, m2–5 retain cusp b, and m3–5 cusp d. Most other cusps are broken or missing, but the preserved parts of these teeth show the clear morphology of *B. serendipitus*, including the distinct a–c crest, and the b–g crest with an absence of the a–g crest on cusp a.

BRSUG 29007 is an incomplete portion of right dentary (Fig. 4F–H). It is broken anteriorly at m1, and posteriorly just posterior to the coronoid scar. It has been extensively worn, although it is unclear whether this occurred as a result of pre-depositional transport, or during field exposure. Due to this wear, molars are identified by size (see Table 1, and Supplementary Information) and remaining morphological features. The posterior root of m1, the roots of m2, m3 to m4, and the roots of m5 and m6, are all present. The crowns of m3–4 are heavily worn, but the presence of a large cusp a lacking an a–g crest and possessing a strong a–c crest can still be distinguished on m4. The presence of these features helps to establish the specimen's identity as *Borealestes serendipitus*.

NMS G.2018.27.1 (Fig. 5) is an almost complete right dentary, still embedded in a small block of limestone matrix (Fig. 5B). The specimen has not been prepared, and only the posteriormost molars protrude from the surface of the block (Fig. 5A). The rest of the dentary is revealed through digital

reconstruction of synchrotron CT scan data. The roots of i2 and i3 remain inside the alveoli, although the incisor crowns are missing, the canine is complete and double-rooted, p1, p2 and p5 are missing but their positions are represented by their alveoli. The posterior root of p3 remains inside the alveolus. The crown of p4 is present, although fractured in the mid-length of the tooth. Of the molars, m1 to m4 are present, and m5 crown is missing but its roots remain in the alveolus. The m3 crown is fractured and displaced, but still identifiable, while m4 is missing cusp a. The molars are otherwise intact, and possess a strong a–c crest and b–e crest, with the a–g crest absent on rounded cusp a: all are diagnostic features of *Borealestes serendipitus.*

NMS G.1992.47.121.3 is an almost complete right mandible (Fig. 6). It belongs to a partial skeleton, NMS G.1992.47.121.1 (currently under study by EP). It is complete except for the apex of the coronoid process and buccal surface of the incisor region. The incisors are missing, but exposed incisor alveoli indicate that the specimen had four incisors, consistent with the count of incisor alveoli in NMS G.2018.27.1 (above). The roots of the canine remain in their alveoli, and the roots and some of the crown of p1 remain. The crowns of the rest of the remaining teeth are well-preserved, except for the missing tips of cusp a of m3 and m4. The molar morphology matches that of the holotype of *Borealestes serendipitus*, with distinct a–c and b–g crests, and an absent a–g crest on the rounded cusp a.

Dentary Morphology

The dentary of *Borealestes serendipitus* is gracile, as exemplified by NMS G.2018.27.1 and NMS G.1992.47.121.3 (Fig. 5, 6), similar to *Agilodocodon* (Meng et al., 2015). The most complete dentary, NMS G.1992.47.121.3, measures 23.3 mm in length from the alveolus of first incisor to the dentary condyle, which represents the complete length of the mandible. The body of the mandible of NMS G.1992.47.121.3 is between 0.9–1.2 mm in buccolingual width, and is 2.2 mm in dorsoventral depth below m3.

The mandibular symphysis of *Borealestes serendipitus* is vertically shallow, but anteroposteriorly long, and is indicated by a slightly rugose area on the medial surface of the dentary (Fig. 5C, 6A). The symphysis begins anteriorly in the incisor region, and continues posteriorly ventral to the canine and posteriorly to below p4–p5. The posterior extension of symphysis is similar to that of *Docodon* (Schultz et al., 2017).

There are three mental foramina on the buccal surface of the dentary, below i3–4, c, and p1, as seen in NMS G. 2018.27.1, NMS G.1992.47.121.3 (Fig. 5C, 6A). In BRSUG 20570 there are also two small nutritive foramina ventral to p5 and to m1, at around midheight dorsoventrally on the buccal surface of the dentary (Fig. 3C).

A very small nutritive foramen is present in the masseteric fossa, as seen in BRSUG 20570, BRSUG 20571, BRSUG 29007 and NMS G.1992.47.121.3 (Fig. 3C, 4B, G, 6B). Its position is low and it is not connected to the masseteric foramen, nor is the masseteric foramen large, unlike in zatherians such as *Peramus* (Davis, 2012). This appears to be a unique feature of *Borealestes*, as

the same foramen is not present in the well preserved mandibles of *Docodon* (Rougier et al., 2015) or other docodonts (Meng et al., 2015).

The V-3 notch is located above the postdentary trough, posterior to the coronoid scar (Fig. 4F, 6A). The postdentary trough is dorsoventrally deep and clearly defined. Within the postdentary trough, there is a well-defined diagonal ridge (sensu Kermack et al., 1973) as in *Morganucodon* (Fig. 6A). The diagonal ridge is much better developed in *Borealestes* here than in *Docodon* (Schultz et al., 2017). There is an angular concavity or notch, for receiving the hook-like reflected lamina of the angular bone, or the ectoympanic 'hook' as in *Castorocauda* and *Agilodocodon* (Ji et al., 2006; Meng et al., 2015).

The dorsal half of the trough is connected anteriorly to the mandibular canal. The mandibular canal is located ventral to the coronoid scar (Fig. 3A, 4A, F, 6A). The canal opening is connected to the postdentary trough in a deep groove defined by the diagonal ridge, best seen in NMS G.1992.47.121.3 (Fig. 6A). In well-preserved specimens, the mandibular canal can be traced inside the dentary, extending along the length of the mandibular body at the base of the tooth roots, on the buccal side of the root tips (Fig. 3G, 4D–E). In BRSUG 20571, a fine vascular network can also be traced posterior to and around the base of m5. This vascular network is near the position of the crypt for m6 in the (likely older) holotype of *Borealestes serendipitus,* BRSUG 20570. We hypothesise this may represent vascularization of the bone prior to the initial formation of the m6 tooth bud.

In BRSUG 29007, the alveolus of m6 is positioned anterior to the anterior margin of the coronoid process. In the growth series of *Docodon* (Schultz et al., 2017:fig 2), the ultimate molar in the juvenile mandible erupts medial to the coronoid process; but in successively older mandibles, the last molar shifts in relative position so that it is anterior to the coronoid process. Based on the shifting placement of the ultimate lower molar(s) in *Docodon*, the placement of the ultimate lower molar directly anterior to the coronoid process of the mandible in BRSUG29007 indicates that this individual of *B. serendipitus* was a fully grown adult.

The Meckel's sulcus is connected to the anterior end of the postdentary trough, and the sulcus starts from below the diagonal ridge and extends anteriorly to below the m4. Further anteriorly, it extends only a millimetre into the medial surface of the dentary. A faint line continues beyond this to the ventral surface of the dentary below m2

The entrance to the mandibular canal is located dorsal to the Meckel's sulcus. The anteriormost extent of Meckel's sulcus varies between specimens, representing ontogenetic change in morphology (see Discussion). In BRSUG20570 the Meckel's sulcus extends from a point ventral to the mandibular canal opening and ends ventral to m3, stopping short of the ventral surface of the dentary. In BRSUG 29007 the Meckel's sulcus extends to a point ventral to m4, where it is reduced to a faint external groove. In NMS G.2018.27.1 the sulcus is open and reaches anteriorly until a point ventral to m4. In all cases, the sulcus

does not continue internally beyond the anteriormost point on the surface of the dentary.

Fragments of Meckel's element remain in the sulcus of all specimens except BRSUG 29007 (Fig. 3A, 4A, 5C, 6A). This is equivalent to the ossified Meckel's cartilage as identified for several extinct clades of crown group mammals (Luo, 2011; Meng et al., 2011). This element was identified as the prearticular in older literature (Kermack et al., 1973; Allin, 1975). As both the prearticular and the Meckel's element are anterior extensions of the articular (= malleus), these are synonymous terms for the homologous structure (Luo et al., 2017). The Meckel's sulcus ends anteriorly below m3, but continues as a faint external groove to meet the ventral surface of the dentary below m1 (Fig. 3A). A fragment of the postdentary complex remains in the post dentary trough in BRSUG 20571.

The anterior margin of the masseteric fossa along the coronoid process is distinct. There is an efflected angle of the angular process. The dentary condyle is a mediolaterally broad, projecting posteriorly on the dentary peduncle. In posterior view, the dentary condyle has a spindle shaped outline (see Supplementary Material). In lateral view, there is a low ridge extending from the dentary condyle along the dentary peduncle anteroventrally into the masseteric fossa (Fig. 6B). This is the lateral ridge, which is interpreted as the demarcation of the superficial masseter below and the deep masseter above (sensu Schultz et al., 2017). The peduncle sits above the line of the toothrow. What remains of the coronoid process is gracile, as is the whole dentary.

There is a strongly projecting medial ridge that overhangs the postdentary trough on the lingual side of the mandible (Fig. 6A). The ridge has a large protuberance, which appears to be curved dorsally, but close examination of the CT scan data shows this to be the result of a fracture along the flat shelf of the medial ridge, which has subsequently been glued into the incorrect anatomical position (EP, pers. obs) (Fig. 6A and Supplementary Material). Therefore we interpret the apparent dorsally curved morphology is an artefact of post-mortem distortion.

The medial ridge ends at the protuberance, and there is a distinct and broad notch between the protuberance and the dentary peduncle, which is termed the medial ridge notch (Fig. 6A). This notch is present in *Docodon* (Schultz et al., 2017), but it appears to be more pronounced in *Borealestes.* The medial ridge lessens at the V3 notch, just posterior to the coronoid scar (Fig. 6A).

BOREALESTES MUSSETTAE Sigogneau-Russell, 2003

Borealestes mussetti Sigogneau-Russell, 2003; Averianov, 2004:3 (emended gender)

Holotype—NHMUK PV M46495 right lower molar from the Forest Marble Formation at Kirtlington, Oxfordshire.

Referred Specimens— NHMUK PV M46224, NHMUK PV M46239; NHMUK PV M46001; NHMUK PV M46066, NHMUK PV M46836, NHMUK PV M46319, NHMUK PV M46809, NHMUK PV M46835, all lower molars, and NHMUK PV M46394, NHMUK PV M46448, NHMUK PV M46580, NHMUK PV

M46871 all upper molars from the Forest Marble Formation at Kirtlington, Oxfordshire. NHMUK PV M46001 lower molar from Watton Cliff, Dorset. (NHMUK PV M46401, NHMUK PV M46389, NHMUK PV M46588 were previously referred to *B. mussettae*, but were re-identified as *B. serendipitus* during present study). NHMUK PV M46404, NHMUK PV M46204 were referred to *B. mussettae,* but lack clear diagnostic features above order-level. Previously assigned to *B.mussettae*, but unavailable for confirmation NHMUK PV M46796.

Revised Diagnosis—Diagnosis for the genus *Borealestes* as for *B. serendipitus* (above). *B. mussettae* (Fig. 7B, D, E) differs from *B. serendipitus* in lower molar morphology in that the a–g crest is present on both cusp g and cusp a, and in having a strong a–d crest on cusp a**—**both features are absent on cusp a in *B. serendipitus*. Cusp g is slightly more developed in *B. mussettae*, and cusps g and c are placed further apart mesiodistally than in *B. serendipitus*. *B. mussettae* has an anterior lingual cingulid that passes below cusp g to the midway along the molar mesiodistally. The df cusp is more developed in *B. mussettae* than in *B. serendipitus,* and is distinct from the d cusp. Cusp e is positioned in alignment with the anteroposterior axis of the molar, whereas cusp e is lingual of the anteroposterior axis on molars of *B. serendipitus* (Fig. 7).

Although *B. mussettae* resembles *B. serendipitus* in most features of upper molars, *B. mussettae* is distinctive in having a more rounded cusp A so that there is no anterior crest and no anterolabial crest on cusp A. *B. mussettae* is also distinguishable from *B. serendipitus* in having a short anterolingual crest on cusp X, with a cuspule on the crest. Cusp Z is reduced to absent relative to *B.*

mussettae. The anterior fovea is less distinct in *B. mussettae* than in *B. serendipitus* (Fig. 7D-E).

DESCRIPTION

The holotype of *B. mussettae*, NHMUK PV M46495, is a lower right molar. Its crown is fractured between cusps a and c on the original specimen, as illustrated by Sigogneau-Russell (2003:fig 2). Here this fracture is digitally restored after segmentation of CT scans (Fig. 7B). Cusp b is missing, but the crown is otherwise intact. The overall morphology of the tooth is more mesiodistally elongate and buccolingually compressed, than in *B. serendipitus*. For molar measurements see Table 1, and Supplementary Material.

Because cusp b is missing, it is not clear how strong the b–g crest is in this specimen. However it is clear that the b–g crest is notched in the depression between these cusps. There is a strong c–d crest on cusp c, although it is less distinctive on cusp d. The c–d crest is posteriorly oriented as in *B. serendipitus*. The a–c crest and the a–d crest are both distinctive, and there is a less distinct a–g crest. The a–g and a–c crests create a mesiodistally flat lingual surface on cusp a, with a faint ridge running from the tip of cusp a to the base dorsoventrally (Fig. 8B1).

Cusp g and cusp c are placed further apart in the holotype of *B. mussettae* than in *B. serendipitus*, leaving a small gap at the base of cusp a that is less distinct to absent in *B. serendipitus*, especially in more posterior molars (Fig. 2

and 7). However, if we are correct that the holotype represents an m1, this gap may not be a feature of the whole tooth row, as we observe a similar larger gap in the m1 of *B. serendipitus* (Fig. 3). Further material is required to resolve this. The anterior lingual cingulid extends posteriorly from cusp e around the base of cusp g to the midpoint of tooth, and terminates ventral to cusp a. Unlike *B. serendipitus*, cusp df is very distinct in *B. mussettae*, projecting further posteriorly and dorsally. The divergent cusps c and g, and the buccolingually compressed crown, are key features of *B. mussettae* distinguishing it from *B. serendipitus*.

RESULTS OF PHYLOGENETIC ANALYSIS

Our analysis includes updated scores for previously missing characters for *Borealestes serendipitus*, described here for the first time. This phylogenetic analysis recovered a single most parsimonious tree of 117 steps (Fig. 8). The topology is almost the same as for Meng et al. (2015), with the following differences: *Morganucodon*, *Megazostrodon* and *Dinnetherium* no longer form a clade, but instead form successive outgroups to the rest of the taxa in the analysis; *Simpsonodon* has become an outgroup to the clade comprising (*Tashkumyrodon* + (*Dsungarodon* + *Castorocauda*), (*Borealestes* + (*Haldanodon* + (*Docodon* + *Docofossor*). *Itatodon* has become an outgroup to the clade comprising (*Krusatodon* + *Agilodocodon*), *Simpsonodon,* (*Tashkumyrodon* + (*Dsungarodon* + *Castorocauda*), (*Borealestes* + (*Haldanodon* + (*Docodon* + *Docofossor*) (Fig. 8). Including *B. mussettae* in the analysis did not alter the tree

topology. *B. serendipitus* and *B. mussettae* are united in the genus *Borealestes*, and *Borealestes* is found as the sister taxon of the clade comprising *Haldanodon*, *Docofossor* and *Docodon*.

Characters recovered as apomorphies of *Borealestes* in this analysis are: character 1, the obtuse angle of the angular process; character 4, the convergence of the Meckel's groove with the ventral margin of the mandible; character 18, cusp c is much larger than cingular cusp g in the lower molars; and 48, the presence of an anterior fovea in the buccolingual midpoint of the upper molar (also present in *Docodon*; Schultz et al., 2017).

Characters recovered as apomorphies of *Borealestes serendipitus* are: character 22, the c–d crest is present and angled; and character 32, the cusp e cingulid being limited to the mesial part of the tooth; character. Characters recovered as apomorphies of *Borealestes mussettae* (lower molar characters only) are: Character 8, the absence of the anterolabial connecting crest on the upper molars; character 19, the pseudo-talonid being bound by the b–e crest; character 20, the presence of an a–g crest with a v-notch; character 21, the weakly developed b–g crest; character 27, presence of an a–d crest connected with a v-notch; character 42, a labially shifted cusp e; and character 44, the broad angle formed by cusps g–a–c (> 80 degrees).

DISCUSSION

Diagnostid Features of *Borealestes*

The new specimens collected from the Kilmaluag Formation on the Isle of Skye, combined with the specimens collected previously, allow us to clarify the diagnoses for *Borealestes serendipitus* and *B. mussettae*. We can confirm that the dental formula for *Borealestes serendipitus* is 4.1.?5.4/ 4.1.5.6. The estimated number of upper premolars will hopefully be clarified by better preserved fossils in the future. Previously referred specimens have been checked in light of this new diagnosis, and the specimen lists herein are up to date.

Borealestes resembles *Krusatodon*, *Castorocauda* and *Haldanodon* in possessing a very large cusp a, and larger cusp c than cusp g. Like most docodonts—except *Simpsonodon, Krusatodon, Agilodocodon,* and *Docodon*—*Borealestes* does not have pits or ornamentation in molar tooth enamel. The key features that distinguish *Borealestes* from other docodonts include: (1) a distinctly pronounced a–c crest; (2) the obtuse angle of the angular process; (3) the convergence of the Meckel's groove with the ventral margin of the mandible; (4) cusp c being much larger than cusp g; (5) and the c–d crest being present and angled; (6) the presence of an anterior fovea in the buccolingual midpoint of the upper molars. However, it should be noted that the angular process and Meckel's groove are not known for *B. mussettae*, and so although these are returned as apomorphies in this analysis, further material is necessary to confirm features (2) and (3) for both taxa.

The differences between *B. serendipitus* and *B. mussettae* are summarised in Figure 8. The species *B. serendipitus* differs from *B. mussettae* in: (1) the

pseudo-talonid being bound by the b–g crest; (2) the better developed b–g crest; (3) the angle formed by cusps g–a–c being < 80 degrees; (4) the presence of the anterolabial and anterolingual crest (the A–X crest) on the upper molars; (5) the reduction/absence of cusp Z; (6) absence of a–g crest on cusp a. The a–d crest and df cusp are better developed, and cusps c and g placed anteroposteriorly further apart in *B. mussettae* than in *B. serendipitus*. Our re-examination of *Borealestes mussettae* shows that it is valid species, and sufficiently different from *B. serendipitus* (further details in Discussion).

Toothrow Size Gradient

The molars of *B. serendipitus* increase in size along the tooth row from m1–m3, then decrease from m3 posteriorly (Table 1, Supplementary). In all docodonts for which the relatively complete tooth rows are known the ultimate molar is smaller than the penultimate molars and the ultimate upper molar is also less symmetrical than preceding molars. The decreasing size from m2–3 through to m5–6 documented in *Borealestes* is similar to the tooth size gradient known for *Haldanodon* (Krusat, 1980; Luo and Martin, 2007), *Docodon* (Jenkins, 1969; Schultz et al., 2017), *Castorocauda* (Ji et al., 2006) and *Agilodocodon* (Meng et al., 2015). However, *Borealestes* shows the steepest gradient for decreasing size toward the posterior molars, of all docodonts. For example, both *Borealestes* and *Docodon* have six molars, but the decreasing trend of m3 to m6 is more pronounced in *Borealestes* (Table 1, Supplementary).

The large sample of specimens of *Borealestes serendipitus* allows a quantitative comparison of *B. serendipitus* to *B. mussettae*. The initial diagnosis and description of *B. mussettae* suggested that *B. mussettae* was larger than *B. serendipitus* (Sigogneau-Russell, 2003:358). Our measurements do not support this, and show instead that specimens of *B. mussettae* are of similar size to *B. serendipitus* (Table 1, Supplementary). The width/length ratio of the type specimen of *B. mussettae* NHMUK PV M46495—a lower molar—is similar to p5 in *B. serendipitus*, but we suggest from the morphology that this specimen represents an m1, suggesting that *B. mussettae* has a buccolingually narrower molar row than *B. serendipitus*.

An alternative hypothesis is that NHMUK PV M46495 could represent a deciduous p5 in *B. serendipitus*. The sharply cusped crown, divergent orientation of cusps c and g (Fig. 7), and the lack of roots in the preserved tooth of *B. mussettae* type specimen could be consistent with the hypothesis that the type specimen is a deciduous dp5. However, the assessment of isolated deciduous premolars without the context of contiguous toothrow can be a complex issue (Averianov, 2004), which can only be resolved reliably when well preserved tooth row is available (Schultz et al., 2017). Much of the material currently referred to *B. mussettae* is fragmentary. More complete specimens of *B. mussettae,* or more juvenile material from *B. serendipitus,* would help resolve this.

Ontogenetic Changes in *Borealestes*

Most of the specimens of *B. serendipitus* found so far have not developed m6 (the ultimate molar) except for the holotype BRSUG 20570 (Fig. 3). A recent detailed analysis of *Docodon victor* shows that its ultimate molar did not erupt until late in adulthood, only in very mature individuals (Schultz et al., 2017). Our observations that *B. serendipitus* also shows a late eruption of m6 suggest this condition of delayed eruption of the ultimate molar may be widespread among docodonts. A corollary of this observation is that the holotype of *Borealestes serendipitus* BRSUG 20570 is the most mature individual of the species currently known.

Other changes in mandibular morphology of *D. victor*, as seen in successively older adult specimens, include a posterior shift in the Meckel's sulcus, a posterior shift in the anterior border of the coronoid process, and a medial-to-anterior shift of the ultimate molar placement relative to the coronoid process (Schultz et al., 2017). The morphology of BRSUG 20570 also conforms to this, further supporting our interpretation that there is some ontogenetic variation in the sample of mandibles of *B. serendipitus* from the Isle of Skye, and that the type specimen BRSUG 20570, and possibly also BRSUG 29007, are the most mature individuals.

Of the other specimens described here, BRSUG 20571 is likely to represent the ontogenetically youngest individual, with the Meckel's sulcus meeting the ventral edge of the mandible below m1 (Fig. 4A–E). In NMS G.2018.27.1 (Fig. 5) and NMS G.1992.47.121.3 (Fig. 6) the anterior end of the Meckel's sulcus has become shorter and ends below m3 and m4, becoming a faint line on the exterior

of mandible anterior to this. Although this posteriorly receding Meckel's sulcus is best documented in *Docodon* (Schultz et al., 2017) it was also previously shown for *Haldanodon* (Nowotny et al., 2001; Martin et al., 2010). This supports the hypothesis that a similar pattern of ontogenetic variation in mandibular morphology may be widespread throughout Docodonta.

Phylogeny of *Borealestes* and Docodonts

Our phylogenetic analysis with updated characters for the upper and lower dentition and dentary of *B. serendipitus* and *B. mussettae* returned similar results to previous analyses of Docodonta (Fig. 8; see Meng et al., 2015). Our analysis continues to support Docodonta as a clade, with *Tikitherium*, *Woutersia* and *Delsatia* as their putative near relatives (Sigogneau-Russell and Hahn, 1995; Ji et al., 2006; Luo and Martin, 2007). *Borealestes* was found to form a clade with *Haldanodon, Docodon and Docofossor*, as recovered by previous authors (Martin and Averianov, 2004; Pfretzschner et al., 2005; Ji et al., 2006; Luo and Martin, 2007; Averianov et al., 2010; Meng et al., 2015). As noted in the description of molars, the posterior upper molar(s) of *Borealestes* bears strong resemblance to the molars of *Haldanodon*, also somewhat similar to those of *Docodon* (although to a lesser extent). These taxa share a relatively strong A–X crest, in perpendicular arrangement to the A–C crest on the upper molars.

The broad agreement of many studies is that there is strong support for the close relationship of *Borealestes* to *Haldanodon, Docodon* and *Docofossor*. However, Sigogneau-Russell (2003) suggested a sister-group relationship

between *Borealestes* + (*Simpsonodon* and *Krusatodon*), based on the morphology of the lower molars. This was an older study, prior to the discoveries of many more docodont taxa. Inclusion of additional taxa has changed the phylogeny. Also the earlier analysis was a manual and ad hoc cladistic phylogeny, not a parsimony analysis with comprehensive coverage of taxa and characters.

Another analysis that returned an alternative placement for *Borealestes* species was Hu et al. (2006). Their analysis of 24 lower molar characters included 13 docodont genera with *Morganucodon* as an outgroup. They found both *Borealestes* species at the base of the docodont tree. Their closest relationship to *Borealestes* was with *Docodon*—and as the outgroup to a clade formed by all other docodonts. Several taxa in this phylogeny are in an unresolved polytomy (Hu et al., 2006:fig 5). The small size of their character list may have contributed to this result, and this earlier study is before our addition of many more characters of *Borealestes* from the new specimens.

Some authors have proposed Docodonta be split into two families: Tegotheriidae (*Tegotherium, Sibirotherium, Hutegotherium* and *Krusatodon*) and Simpsonodontidae (*Simpsonodon* and *Dsungarodon*), with basal docodonts represented by *Borealestes, Haldanodon* and *Docodon* (Maschenko et al.,2002; Martin and Averianov 2004; Averianov et al., 2010). This was based on an analysis of 37 molar and dentary characters scored for 18 taxa, 13 of them docodonts. In the resulting tree, *Borealestes*, plus *Haldanodon* and *Docodon* were placed in an unresolved polytomy with *Castorocauda, Tashkumyrodon*, and

a clade formed by the rest of Docodonta except *Itatodon*, which formed the outgroup to all other docodonts (Averianov et al., 2010:fig 6). They considered *Castorocauda, Tashkumyrodon* and *Acuoduolodon* to be Docodonta incertae sedis (*Acuoduolodon sunae* has since been suggested to be a junior synonym of *Dsungarodon zoui* [Martin et al., 2010]).

Our analysis does not fully support the dichotomous relationships of families Tegotheriidae and Simpsonodontidae as hypothesized by Averianov et al. (2010). Although there is support for Tegotheriidae comprising *Tegotherium, Sibirotherium* and *Hutegotherium*, we find *Krusatodon* as the sister taxon to *Agilodocodon* outside of this clade (Fig. 8). We also find *Simpsonodon* as an outgroup to two clades formed by *Tashkumyrodon* + (*Dsungarodon and Castorocauda*), and the clade of *Borealestes* + (*Haldanodon* + (*Docodon and Docofossor*)), which has been corroborated by multiple previous analyses. 'Simpsonodontidae' has therefore become paraphyletic in our analysis.

All of these studies are based on molar, or molar plus dentary, morphological characters, without postcrania. This is due to the lack of postcranial material for many docodontans. The addition of postcrania to a phylogenetic analysis would undoubtedly help further resolve and stabilize docodont relationships.

ACKNOWLEDGMENTS

We would like to thank the John Muir Trust and Scottish Natural Heritage for permission to carry out field work on the SSSI site on the Isle of Skye, and our dedicated field work teams for their efforts yearly in collecting specimens. The 2016 field work was supported by a grant from the John Fell Fund of the University of Oxford to RBJB. We are indebted to the Natural Science Department at NMS for access to their fossils and facilities, and ongoing support and collaboration on material from the Kilmaluag Formation. Many thanks to J. Hanson at the BRSUG for arranging loan of their specimens, to the University of Bristol Palaeobiology Research Group for access to their CT scan facilities, and to T. Davies for technical assistance with scanning. Thanks Vincent Fernandez for obtaining synchrotron scan data. EP was funded by NERC (NE/L002558/1), and by The Palaeontolographical Society's Richard Owen Fund. Thanks to N. Fraser and S. Walsh (NMS) for ongoing pastoral and academic support, and to S. Brusatte. ZXL has been supported by Division of Biological Sciences of the University of Chicago, during this research he benefited from the access to comparative fossil collections provided by T. Martin (University of Bonn), Director Q-J. Meng (Beijing Museum of Natural History) and C-F. Zhou and G. Sun (Paleontological Museum of Liaoning). We would like to thank A. Averianov and an anonymous reviewer for their constructive comments and suggestions in review, which helped improve this manuscript.

ORCID

Elsa L. Panciroli https://orcid.org/0000-0001-8350-3380

Roger B. J. Benson https://orcid.org/0000-0001-8244-6177

Zhe-Xi Luo https://orcid.org/0000-0003-2170-8879

LITERATURE CITED

Allin, E. F. 1975. Evolution of the mammalian middle ear. Journal of Morphology 147:403–438.

Andrews, J. E. 1985. The sedimentary facies of a late Bathonian regressive episode: the Kilmaluag and Skudiburgh Formations of the Great Estuarine Group, Inner Hebrides, Scotland. Journal of the Geological Society of London 142:1119–37.

Anquetin, J. E. 2009. A new stem turtle from the Middle Jurassic of Scotland: new insights into the evolution and palaeoecology of basal turtles. Proceedings of the Royal Society B 276:879–886.

Anquetin, J. E. 2010. The anatomy of the basal turtle *Eileanchelys waldmani* from the Middle Jurassic of the Isle of Skye, Scotland. Earth and Environmental Science Transactions of the Royal Society of Edinburgh 101:67–96.

Averianov, A. O. 2004. Interpretation of the Early Cretaceous mammal *Peraiocynodon* (Docodonta) and taxonomy of some British Mesozoic docodonts. Russian Journal of Theriology 3:1–4.

Averianov, A. O., and A. V. Lopatin. 2006. *Itatodon tatarinov* (Tegotheriidae, Mammalia), a docodont from the Middle Jurassic of western Siberia and phylogenetic analysis of Docodonta. Paleontological Journal 40:668–677.

Averianov, A. O., A. V. Lopatin, S. A. Krasnolutskii, and S. V. Ivantsov. 2010. New docodontans from the Middle Jurassic of Siberia and reanalysis of Docodonta interrelationships. Proceedings of Zoological Institute of Russian Academy of Sciences 314:121–148.

Barrett, P. M. 2006. A sauropod dinosaur tooth from the Middle Jurassic of Skye, Scotland. Transactions of the Royal Society of Edinburgh Earth Sciences 97:25–29.

Barron, A. J. M., G. K. Lott, and J. B. Riding. 2012. Stratigraphical framework for the Middle Jurassic strata of Great Britain and the adjoining continental shelf. British Geological Survey Research Report, RR/11/06. British Geological Survey, Keyworth.

Chen, P.-J., and J. D. Hudson. 1991. The chonchostracan fauna of the Great Estuarine Group, Middle Jurassic, Scotland. Palaeontology 34:515–545.

Close, R. A., B. M. Davis, S. Walsh, A. S., Woloniewicz, M. Friedman, and R. B. J. Benson. 2015. A lower jaw of *Palaeoxonodon* from the Middle Jurassic of the Isle of Skye, Scotland, sheds new light on the diversity of British stem therians. Palaeontology 59:155–169.

Datta, P.M. 2005. Earliest mammal with transversely expanded upper molar from the Late Triassic (Carnian) Tiki Formation, South Rewa Gondwana Basin, India. Journal of Vertebrate Paleontology 25: 200–207.

Davis, B. M. 2012. Micro-computed tomography reveals a diversity of peramuran mammals from the Purbeck Group (Berriasian) of England. Palaeontology 55:789–817.

Evans, S. E. 1992. Small reptiles and amphibians from the Forest Marble (Middle Jurassic) of Dorset. Proceedings of the Dorset Natural History and Archaeological Society 113:201–202.

Evans, S. E., and A. R. Milner. 1994. Middle Jurassic microvertebrate assemblages from the British Isles; pp. 303–321 in N. C. Fraser. and H. Sues (eds.), In the Shadow of the Dinosaurs: Early Mesozoic Tetrapods. Cambridge University Press, Cambridge.

Evans, S. E., P. M. Barrett, J. Hilton, R. J. Butler, M. E. H. Jones, M.-M. Liang, J. C. Parish, E. J. Rayfield, D. Sigogneau-Russell, and C. J. Underwood. 2006. The Middle Jurassic vertebrate assemblage of Skye, Scotland; pp. 36–39 in P. M. Barrett, and S. E. Evans (eds.), The 9th International Symposium on Mesozoic Terrestrial Ecosystems and Biota, Abstracts and Proceedings Volume, Natural History Museum, London.

Freeman, E. F. 1979. A Middle Jurassic mammal bed from Oxfordshire. Palaeontology 22:135–166.

Gill, P. G. 2004. *Kuehneotherium* from the Mesozoic fissure fillings of South Wales. Ph.D. dissertation, University of Bristol, 285pp. (Open Access: https://research-information.bristol.ac.uk/files/34500808/424430.pdf)

Gingerich, P. D. 1973. Molar occlusion and function in the Jurassic mammal *Docodon*. Journal of Mammalogy 254:1008–1013.

Holloway, S. 1983. The shell-detrital calcirudites of the Forest Marble Formation (Bathonian) of South West England. Proceedings of the Geological Association 94:259–266.

Hopson, J. A., and A. W. Crompton. 1969. Origin of mammals; pp. 15–72 in: T Dobzhansky M. K. Hecht, and W. C. Steere (eds.), Evolutionary Biology, Volume 3. Appleton-Century-Crofts, New York.

Hudson, J. D. 1980. Aspects of brackish-water facies and faunas from the Jurassic of north-west Scotland. Proceedings of the Geologists' Association 91:99–105.

Jenkins, F. A., Jr. 1969. Occlusion in *Docodon* (Mammalia, Docodonta). Postilla 139:1–24.

Ji, Q., Z.-X. Luo, C.-X. Yuan, and A. R. Tabrum. 2006. A swimming mammaliaform from the Middle Jurassic and ecomorphological diversification of early mammals. Science 311:1123–1127.

Kermack, K. A. 1988. British Mesozoic mammal sites. Special papers in Palaeontology 40:85–93.

Kermack, K. A., F. Mussett, and H. W. Rigney. 1973. The lower jaw of *Morganucodon*. Zoological Journal of the Linnean Society 53:87–175.

Kielan-Jaworowska, Z., R. L. Cifelli, and Z.-X. Luo. 2004. Mammals from the age of dinosaurs: origins evolution and structure. Columbia University Press, New York, N.Y., 630 pp.

Kretzoi, M. 1946. On Docodonta, a new order of Jurassic mammals. Anneles Historico-Naturales Musei Nationalis Hungarici 39:108–111.

Krusat, G. 1980. Contribuçao para o conhecimento da fauna do Kimeridgiano da mina de lignito Guimarota (Leiria, Portugal). IV Parte. *Haldanodon exspectatus* Kuhne & Krusat 1972 (Mammalia, Docodonta). Memorials dos Serviços Geologicos de Portugal 27:1–79.

Lillegraven, J. A., and G. Krusat 1991. Cranio-mandibular anatomy of *Haldanodon exspectatus* (Docodonta; Mammalia) from the Late Jurassic of Portugal and its implications to the evolution of mammalian characters. Contributions to Geology, University of Wyoming 28:39–138.

Lopatin, A. V., and A. O. Averianov. 2005. A new docodont (Docodonta, Mammalia) from the Middle Jurassic of Siberia. Dokaldy Biological Sciences, 405:434–436.

Luo, Z.-X. 1994 Sister taxon relationships of mammals and the transformation of the diagnostic mammalian characters; pp. 98–128, in N. C. Fraser, and H.-D. Sues (eds.), In the Shadow of Dinosaurs: Early Mesozoic Tetrapods. Cambridge University Press, Cambridge and New York.

Luo, Z.-X. 2011. Developmental patterns in Mesozoic evolution of mammal ears. Annual Reviews of Ecology, Evolution and Systematics 42:355–80.

Luo, Z.-X., Kielan-Jaworowska, Z., and R. L. Cifelli. 2002. In quest for a phylogeny of Mesozoc mammals. Acta Palaeontological Polonica 47:1–78.

Luo Z.-X., Kielan-Jaworowska, Z., and R. L. Cifelli. 2004. Evolution of dental replacement in mammals. Bulletin of the Carnegie Museum of Natural History 36:159–175.

Luo Z.-X., and T. Martin. 2007. Analysis of molar structure and phylogeny of docodont genera. Bulletin of the Carnegie Museum of Natural History 39:27–47.

Luo, Z.-X. S. M. Gatesy, S. M., F. A. Jenkins, Jr., A. A. Amaral, and N. H. Shubin. 2015a. Mandibular and dental characteristics of Late Triassic mammaliaform *Haramiyavia* and their ramifications for basal mammal evolution. Proceedings of the National Academy of Sciences 112:E7101–E7109.

Luo, Z.-X., Q.-J. Meng, Q. Ji, D. Liu, Y. Zhang, and A. I. Neander. 2015b. Evolutionary development in basal mammaliaforms as revealed by a docodontan. Science 347:760–764.

Luo, Z.-X., Q.-J., Meng, D. M. Grossnickle, D. Liu, Y.-G. Zhang, A. I. Neander, and Q Ji. 2017. New evidence for mammaliaform ear evolution and feeding adaptation in a Jurassic ecosystem. Nature 548:326–329.

Marsh, O. C. 1887. American Jurassic Mammals. American Journal of Science 33:326-348.

Martin, T. 2005. Postcranial anatomy of *Haldanodon exspectatus* (Mammalia, Docodonta) from the Late Jurassic (Kimmeridgian) of Portugal and its bearing for mammalian evolution. Zoological Journal of the Linnean Society 145:219–248.

Martin, T., and A. O. Averianov. 2004. A new docodont (Mammalia) from the Middle Jurassic of Kyrgyzstan, Central Asia. Journal of Vertebrate Palaeontology 30:855–871.

Martin, T., and M. Nowotny. 2000. The docodont *Haldanodon* from the Guimarota mine; pp. 91–96, in T. Martin and B. Krebs (eds.), Guimarota: a Jurassic Ecosystem. Verlag Dr. Friedrich Pfeil, München.

Martin, T., M. Nowotney, and M. Fischer. 2010. New data on tooth replacement in the Late Jurassic docodont mammal *Haldanodon exspectatus*. Society of Vertebrate Paleontology 70th Annual Meeting. Program and Abstracts:130A.

Maschenko, E. N., A. V. Lopatin, and A. V. Voronkevich. 2002. A new genus of tegotheriid docodonts (Docodonta, Tegotheriidae) from the Early Cretaceous of west Siberia. Russian Journal of Theriology 1:75–81.

Meng, J., Y.-Q. Wang, and C. Li. 2011. Transitional mammalian middle ear from a new Cretaceous Jehol eutriconodont. Nature 472:181–185.

Meng, Q.-J., Q. Ji, Y. Zhang, D. Liu, D. M. Grossnickle, and Z.-X. Luo. 2015. An arboreal docodont from the Jurassic and mammaliaform ecological diversification. Science 347:760–764.

Morton, N., and J. D. Hudson. 1995. Field guide to the Jurassic of the Isles of Raasay and Skye, Inner Hebrides, NW Scotland; pp. 209–280 in P.D. Taylor (ed.), Field Geology of the British Jurassic. Geological Society, London.

Nowotny, M., T. Martin, and M. S. Fischer. 2001. Dental anatomy and tooth replacement of *Haldanodon exspectatus* (Docodonta, Mammalia) from the Upper Jura of Portugal. Journal of Morphology 248:268.

Panciroli, E., R. B. J. Benson, and S. Walsh. 2017a. The dentary of *Wareolestes rex* (Megazostrodontidae): a new specimen from Scotland and implications

for morganucodontan tooth replacement. Papers in Palaeontology 3:373–386.

Panciroli, E., S. Walsh, N. Fraser, S. L. Brusatte, and I. Corfe. 2017b. A reassessment of the postcanine dentition and systematics of the tritylodontid *Stereognathus* (Cynodontia, Tritylodontidae, Mammaliamorpha), from the Middle Jurassic of the UK. Journal of Vertebrate Paleontology 3:373–386.

Panciroli, E., J. A. Schultz, and Z.–X. Luo. 2018a. The morphology of the petrosal and stapes of *Borealestes* (Mammaliaformes, Docodonta) from the Middle Jurassic of Skye, Scotland. Papers in Palaeontology https://doi.org/10.1002/spp2.1233

Panciroli, E., R. B. J. Benson, and R. J. Butler. 2018a. New partial dentaries of *Palaeoxonodon ooliticus* (Mammalia, Amphitheriidae) from Scotland, and posterior dentary morphology in stem cladotherians. Acta Paleontologica Polonica 63:197–206.

Pfretzschner, H. U., T. Martin, A. T. Matzke, and G. Sun. 2005. A new docodont mammal from the Late Jurassic of the Junggar Basin in Northwest China. Acta Palaeontologica Polonica 50:799–808.

Prasad, G. V. R., and B. K. Manhas. 2001. First docodont mammals of Laurasian affinities from India. Current Science 81:1235–1238.

Prasad, G. V. R., and B. K. Manhas. 2007. A new docodont mammal from the Jurassic Kota Formation of India. Palaeontologia electronica 10.2:1–11.

Rougier, G. W., A. S. Sheth, K. Carpenter, L. Appella-Guiscafre, and B. M. Davis.

2015. A new species of *Docodon* (Mammaliaformes: Docodonta) from the Upper Jurassic Morrison Formation and a reassessment of selected craniodental characters in basal mammaliaforms. Journal of Mammalian Evolution 22:1–16.

Rowe, T. 1988. Definition, diagnosis, and origin of Mammalia. Journal of Vertebrate Paleontology 8:241–264.

Schultz, J. A., B.-A. S. Bhullar, and Z.-X. Luo. 2017. Re-examination of the Jurassic Mammaliaform *Docodon victor* by computed tomography and occlusal functional analysis. Journal of Mammalian Evolution. https://doi.org/10.1007/s10914-017–9418.

Sigogneau-Russell, D. 2003. Docodonts from the British Mesozoic. Acta Palaeontologica Polonica 48:357–374.

Sigogneau-Russell, D., and R. Hahn. 1995. Reassessment of the Late Triassic symmetrodont mammal *Woutersia*. Acta Palaeontologica Polonica 40:245–260.

Sigogneau-Russell, D., and P. Godefroit. 1997. A primitive docodont (Mammalia) from the Upper Triassic of France and the possible therian affinities of the order. Comptes-Rendus de l'Académie des Sciences, Paris, sér. IIa 324:135–140.

Simpson, G. G. 1929. American Mesozoic Mammalia. Memoirs of Peabody Museum, Yale University 3:1–235.

Wakefield, M. I. 1995. Ostracod biostratinomy at lagoonal shorelines: examples from the Great Estuarine Group, Middle Jurassic, Scotland. Proceedings of the Geologists' Association, 106:211–218.

Waldman, M., and R. J. G. Savage. 1972. The first Jurassic mammal from Scotland. Journal of the Geological Society of London 128:119–125

Wible, J. R., and J. A. Hopson. 1993. Basicranial evidence for early mammal phylogeny; pp. 45–62 in F. S. Szalay, M. J. Novacek, and M. C. McKenna (eds.), Mammal Phylogeny (Volume 1): Mesozoic Differentiation, Multituberculates, Early Therians, and Marsupials. Springer-Verlag, New York.

Wills, S, P. M. Barrett, and A. Walker. 2014. New dinosaur and crocodylomorph material from the Middle Jurassic (Bathonian) Kilmaluag Formation, Skye, Scotland. Scottish Journal of Geology 50:183–190.

Xu, X., Z. Zhou C. Sullivan, and Y. Wang. 2017. The Yanliao Biota: a trove of exceptionally preserved Middle-Late Jurassic terrestrial life forms; pp. 131–167 in N. C. Fraser and H.-D. Sues (eds.), Terrestrial Conservation Lagerstätten. Dunedin Academic Press, London.

Submitted April 16, 2019; accepted Month DD, YYYY

FIGURE 1. Terminology of molar and mandibular morphologies of *Borealestes*. **A,** lower molar cusp terminology (left molar): **A1,** occlusal; **A2,** occlusal diagrammatic; **A3,** lingual view. Lower molar crest terminology: **A4,** occlusal; **A5,**

occlusal diagrammatic; **A6,** lingual view. **B,** upper molar cusp terminology (right molar): **B1,** occlusal; **B2,** occlusal diagrammatic. Upper molar crest terminology: **B3,** occlusal; **B4,** occlusal diagrammatic. **C,** molar measurements (measurements listed in Table 1): **C1**, lower molar measurements; **C2**, upper molar measurements. Figures based on lower m3 of holotype BRSUG 20570, and upper M3 of NMS G.1992.47.121.1. **D,** restoration of complete mandible in medial view; **E,** restoration of mandible in buccal view. **D** and **E** based on composite of specimens herein, incisors in dash-outline based on *Agilodocodon.* [Intended for page width 183 mm]

FIGURE 2. *Borealestes serendipitus* upper dentition. Composite upper tooth row from NMS G.1992.47.121.1 (molars and premolars), and from NMS G.1992.47.121.4 (incisors). **A1,** right tooth row occlusal view; **A2,** left tooth row occlusal view; **B1**, left tooth row lingual view; **B2,** left tooth row buccal view; **C1,** right tooth row lingual view; **C2,** right tooth row buccal view. Digital reconstructions from micro CT scans. Letters in grey color indicate tooth positions represented by empty alveoli of lost teeth. Arrows in bold indicate anterior direction. All scale bars equal 1 mm. [Intended for page width 183 mm]

FIGURE 3. *Borealestes serendipitus* BRSUG 20570 (holotype), partial left dentary. **A,** lingual; **B,** anterolingual; **C**, buccal; **D,** occlusal views of the dentary and dentition; **E,** posterolingual view showing the opening for mandibular canal and relationship to postdentary trough; **F,** micro CT scan slice showing the possible overgrowth of m5 roots suggesting pre-mortem tooth loss; **G,** buccal

view of dentary semi-transparent with segmented mandibular nerve and vessel pathway inside the dentary. Digital reconstructions from micro CT scans. Arrows in bold indicate anterior direction. Scale bar same for **A–D** and **G**. All scale bars equal 1 mm. [Intended for page width 183 mm]

FIGURE 4. *Borealestes serendipitus* BRSUG 20571 (partial left dentary), and BRSUG 29007 (partial right dentary). **A,** lingual; **B,** buccal; **C,** occlusal views of the dentary and dentition of BRSUG 20571. **D,** lingual; and **E,** buccal views of the dentary semi-transparent with segmented mandibular nerve and vessel pathway inside the dentary of BRSUG 20571. **F,** lingual; **G**, buccal; and **H,** occlusal views of the dentary and dentition BRSUG 29007. Digital reconstructions from micro CT scans. Arrows in bold indicate anterior direction. Same scale throughout. All scale bars equal 1 mm. [Intended for page width 183 mm]

FIGURE 5. *Borealestes serendipitus* NMS G.2018.27.1, partial right dentary. **A,** the jaw of NMS G.2018.27.1 as found in situ; **B,** digital reconstruction of dentary in matrix, showing original breakage at p4. Dentary reconstructed from micro CT scans and anterior and posterior portions re-aligned: **C,** lingual; **D,** occlusal; and **E,** buccal view of the dentary and dentition. Letters in grey color indicate tooth positions represented by empty alveoli of lost teeth. Arrows in bold indicate anterior direction. Same scale for **C**–**E**. All scale bars equal 1 mm. [Intended for page width 183 mm]

FIGURE 6. *Borealestes serendipitus* NMS G.1992.47.121.3, almost complete right dentary. **A**, lingual; **B**, buccal; **C**, occlusal views of dentary and dentition. Digital reconstructions from micro CT scans. Arrows in bold indicate anterior direction. Scale same throughout. All scale bars equal 1 mm. [Intended for page width 183 mm]

FIGURE 7. Distinguishing characters of *Borealestes serendipitus* and *B. mussettae.* **A,** and **B,** lower molar characters. **A,** *Borealestes serendipitus* based on m1 of holotype BRSUG 20570: **A1,** lingual; **A2,** occlusal; **A3,** buccal; **A4,** anterior; and **A5,** posterior views of molar. All **B**, *B. mussettae* based on holotype NHMUK PV M46495, but crack through cusp a is repaired, and molar mirrored to facilitate comparison: **B1,** lingual; **B2**, occlusal; **B3**, buccal; **B4**, anterior; and **B5**, posterior views of molar. **C, D** and **E,** distinctive upper molar characters for each species of *Borealestes*: **C**, M3 of *B. serendipitus*, NMS G.1992.47.121.1; **D**, *B. mussettae*, NHMUK PV M46871; **E,** *B. mussettae*, NHMUK PV M46871 anterior view. **D** and **E** mirrored to facilitate comparison. Digital reconstructions from micro CT scans. Dotted lines indicate missing portions of tooth. Arrows in bold indicate anterior direction. Same scale for **A**–**B**, and same scale for **C**–**E**. All scale bars equal 1 mm. [Intended for page width 183 mm]

FIGURE 8. Phylogeny of docodonta, with tree-topology based on updated phylogenetic analysis. Results of parsimony branch and bound analysis of docodonts and outgroups, tree of 117 steps. First to last appearances are

represented by black box for each taxon (for sources of FAD/LADs see Methods). Nodes uniting taxa do not imply divergence times. [Intended for page width 183 mm]

TABLE 1: Measurements of *Borealestes* lower dentition. Measurements in italics are from broken specimens. Dashes indicate missing teeth or tooth portions prevented measurement from being taken. See Figure 1 for measurement methodology.

	All in mm		c	pm1	pm2	pm3	pm4	pm5	m1/ M1	m2/ M2	m3/ M3	m4/ M4	m5/ M5	m6
BRSUG 20570	Length	d to b	-	0.97	1	1.2	0.97	1	1.2	1.32	1.32	1.2	-	0.61
		df to e	-	0.97	1	1.19	0.97	1	1.19	1.33	1.29	1.17	-	0.55
	Width	cross c	-	-	-	-	0.45	0.45	0.65	0.79	0.8	0.74	-	0.36
		cross g	-	-	-	-	0.45	0.45	0.57	0.76	0.84	0.82	-	0.37
BRSUG 20571	Length	d to b	-	-	-	-	-	-	-	1.66	1.67	1.37	0.81	-
		df to e	-	-	-	-	-	-	-	1.6	1.6	1.37	0.78	-
	Width	cross c	-	-	-	-	-	-	-	-	*0.94*	0.73	0.42	-
		cross g	-	-	-	-	-	-	-	-	0.99	0.86	0.56	-
BRSUG 29007	Length	d to b	-	-	-	-	-	-	-	-	*1.37*	*1.35*	-	-

TABLE 1. (Continued)

		df to e	-	-	-	-	-	-	-	-	*1.42*	*1.36*	-	-
	Width	cross c	-	-	-	-	-	-	-	-	*0.66*	*0.67*	-	-
		cross g	-	-	-	-	-	-	-	-	*0.59*	*0.64*	-	-
NMS	Length	d to b	-	-	0.84	1.04	1.15	1.25	1.38	1.47	1.5	1.33	0.93	-
G.1992.47.121.3		df to e	-	-	0.84	1.04	1.15	1.25	1.35	1.41	1.49	1.31	0.85	-
	Width	cross c	-	*0.36*	0.39	0.42	0.46	0.48	0.79	0.89	0.97	0.78	0.43	-
		cross g	-	*0.36*	0.39	0.42	0.46	0.48	0.69	0.83	0.92	0.83	0.57	-
NMS G.2018.27.1	Length	d to b	0.9	-	-	-	1.1	-	1.25	1.34	*1.35*	*1.5*	-	-
		df to e	0.9	-	-	-	1.1	-	1.22	1.33	*1.31*	-	-	-
	Width	cross c	0.41	-	-	-	0.5	-	0.63	0.83	0.87	0.86	-	-
		cross g	0.41	-	-	-	0.5	-	0.56	0.76	*0.84*	-	-	-
NHMUK PV M46495	Length	d to b	-	-	-	-	-	-	1.51	-	-	-	-	-
(*B. mussetti*)		df to e	-	-	-	-	-	-	1.57	-	-	-	-	-
	Width	cross c	-	-	-	-	-	-	0.67	-	-	-	-	-
		cross g	-	-	-	-	-	-	0.58	-	-	-	-	-

TABLE 1. (Continued)

NMS G.1992.47.121.1 (*B. serendipitus*)	Right tooth row	Length	buccal	-	-	-	-	-	-	-	1.6	1.17	-	-
			lingual	-	-	-	-	-	0.81	0.98	0.95	0.7	-	-
		Width		-	-	-	-	-	*1.4*	1.6	1.67	1.41	-	-
	Left tooth row	Length	buccal	-	-	-	-	-	-	-	1.42	1.18	-	-
			lingual	-	-	-	-	-	0.77	0.9	0.93	0.7	-	-
		Width		-	-	-	-	-	1.77	1.63	1.39	1.77	-	-

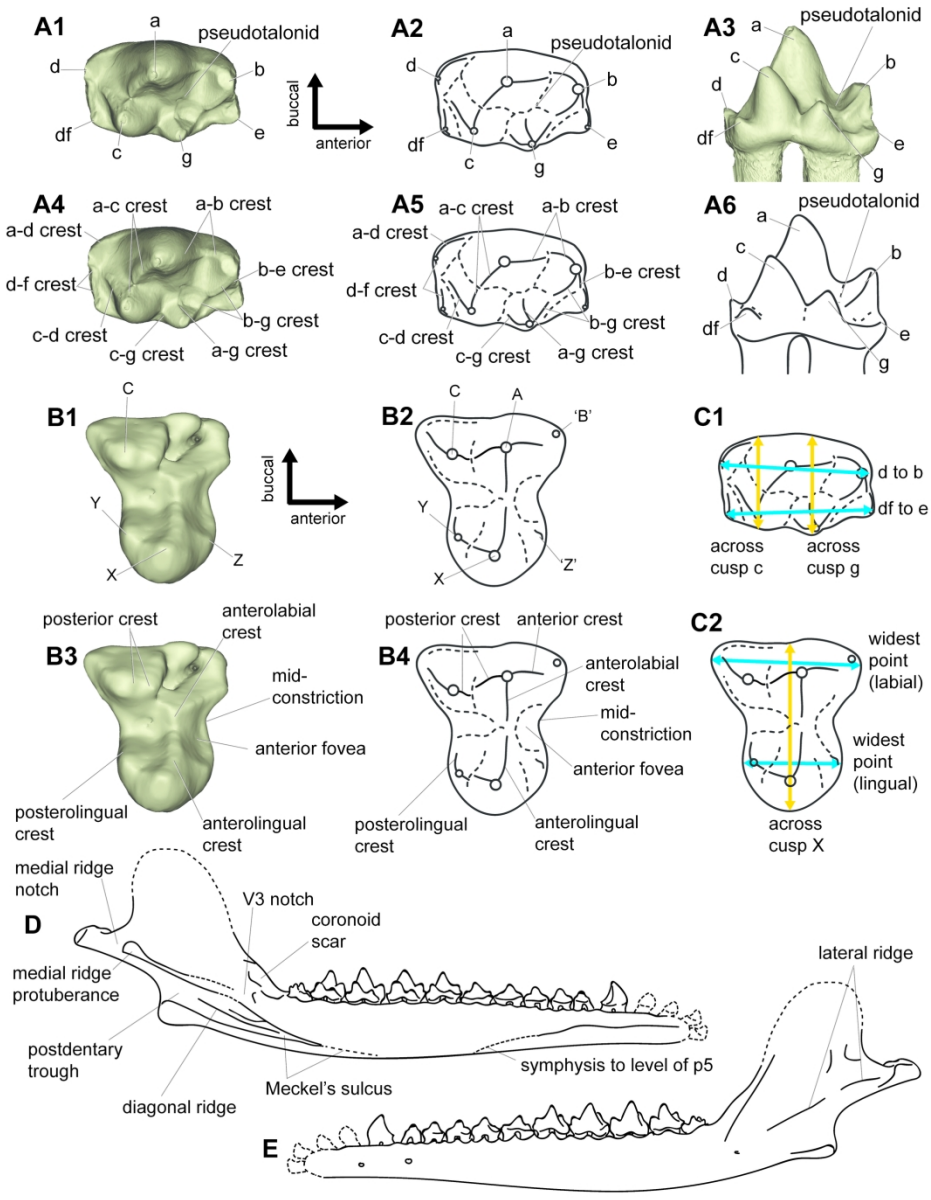

FIGURE 1. Terminology of molar and mandibular morphologies of *Borealestes*. A, lower molar cusp terminology (left molar): A1, occlusal; A2, occlusal diagrammatic; A3, lingual view. Lower molar crest terminology: A4, occlusal; A5, occlusal diagrammatic; A6, lingual view. B, upper molar cusp terminology (right molar): B1, occlusal; B2, occlusal diagrammatic. Upper molar crest terminology: B3, occlusal; B4, occlusal diagrammatic. C, molar measurements (measurements listed in Table 1): C1, lower molar measurements; C2, upper molar measurements. Figures based on lower m3 of holotype BRSUG 20570, and upper M3 of NMS G.1992.47.121.1. D, restoration of complete mandible in medial view; E, restoration of mandible in buccal view. D and E based on composite of specimens herein, incisors in dash-outline based on *Agilodocodon*. [Intended for page width 183 mm]

182x232mm (300 x 300 DPI)

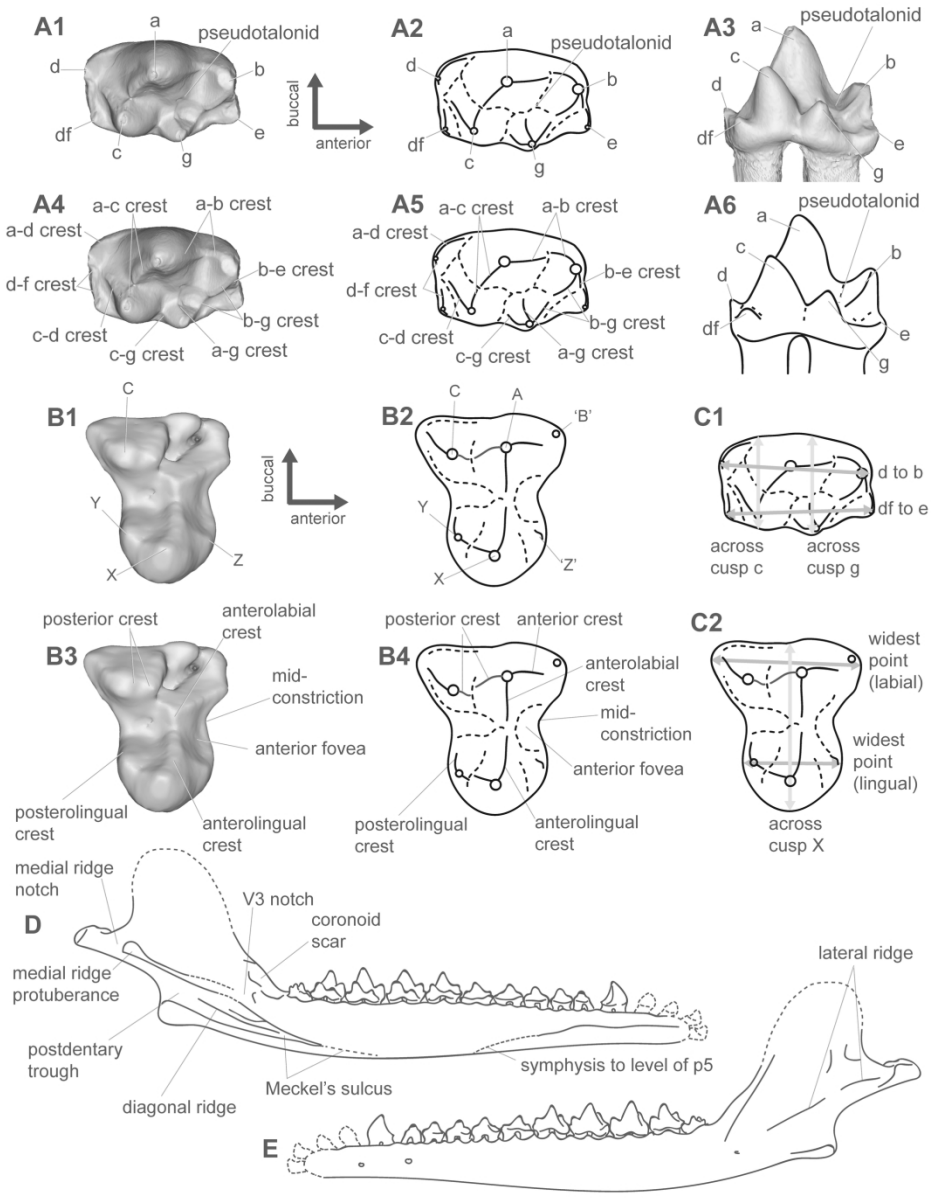

FIGURE 1. Terminology of molar and mandibular morphologies of *Borealestes*. A, lower molar cusp terminology (left molar): A1, occlusal; A2, occlusal diagrammatic; A3, lingual view. Lower molar crest terminology: A4, occlusal; A5, occlusal diagrammatic; A6, lingual view. B, upper molar cusp terminology (right molar): B1, occlusal; B2, occlusal diagrammatic. Upper molar crest terminology: B3, occlusal; B4, occlusal diagrammatic. C, molar measurements (measurements listed in Table 1): C1, lower molar measurements; C2, upper molar measurements. Figures based on lower m3 of holotype BRSUG 20570, and upper M3 of NMS G.1992.47.121.1. D, restoration of complete mandible in medial view; E, restoration of mandible in buccal view. D and E based on composite of specimens herein, incisors in dash-outline based on *Agilodocodon*. [Intended for page width 183 mm]

182x232mm (300 x 300 DPI)

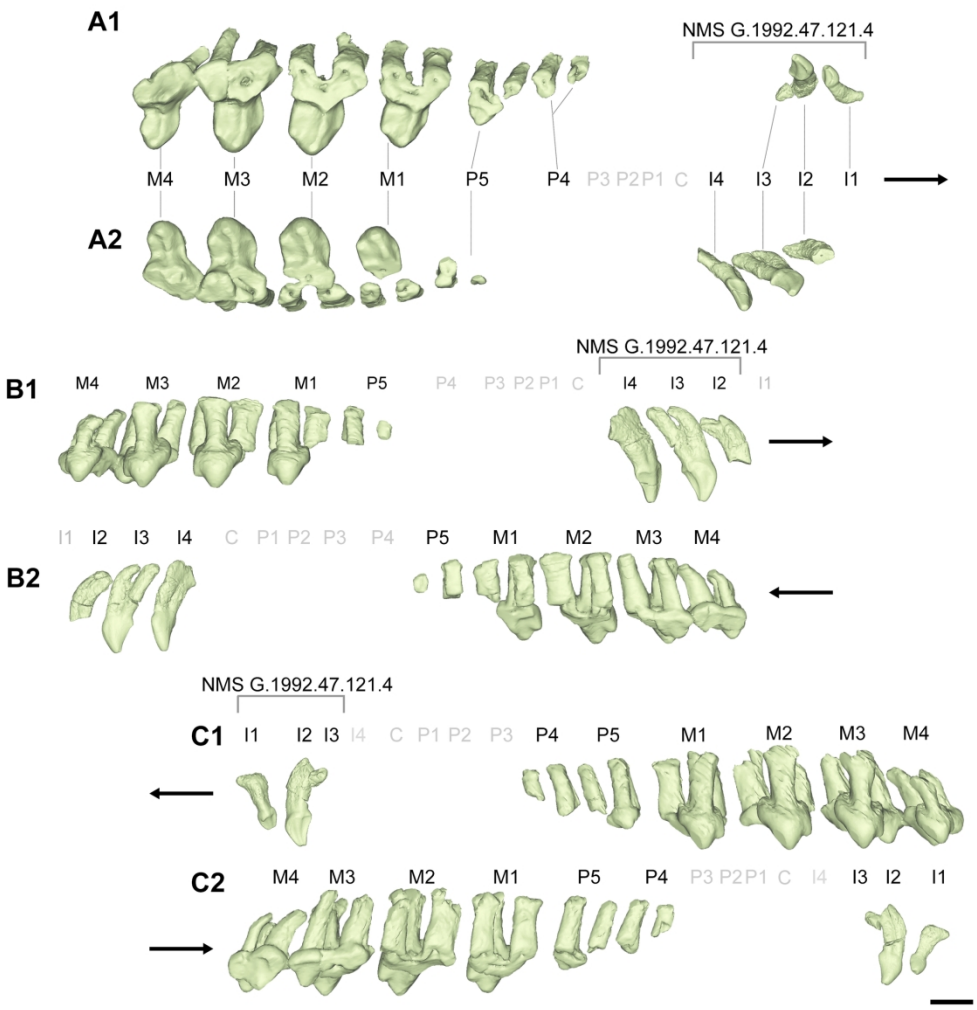

FIGURE 2. *Borealestes serendipitus* upper dentition. Composite upper tooth row from NMS G.1992.47.121.1 (molars and premolars), and from NMS G.1992.47.121.4 (incisors). A1, right tooth row occlusal view; A2, left tooth row occlusal view; B1, left tooth row lingual view; B2, left tooth row buccal view; C1, right tooth row lingual view; C2, right tooth row buccal view. Digital reconstructions from micro CT scans. Letters in grey color indicate tooth positions represented by empty alveoli of lost teeth. Arrows in bold indicate anterior direction. All scale bars equal 1 mm. [Intended for page width 183 mm]

182x187mm (300 x 300 DPI)

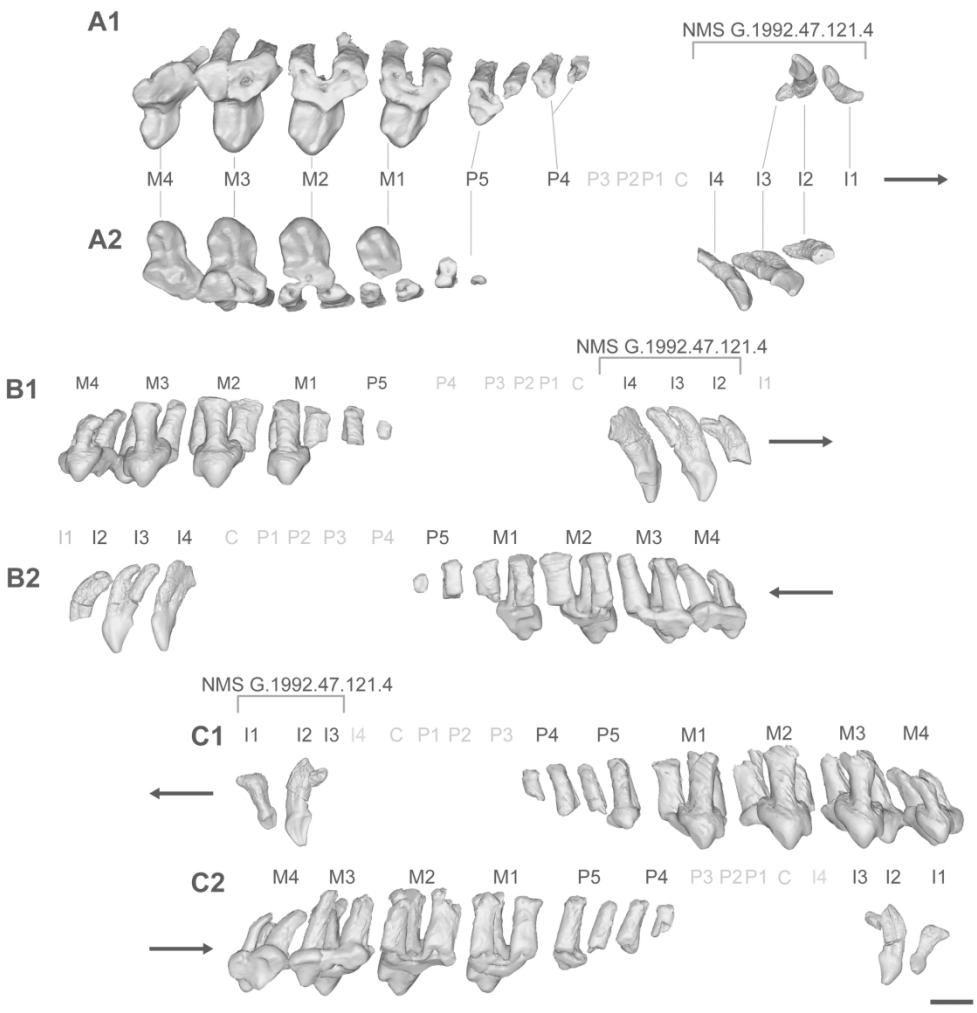

FIGURE 2. *Borealestes serendipitus* upper dentition. Composite upper tooth row from NMS G.1992.47.121.1 (molars and premolars), and from NMS G.1992.47.121.4 (incisors). A1, right tooth row occlusal view; A2, left tooth row occlusal view; B1, left tooth row lingual view; B2, left tooth row buccal view; C1, right tooth row lingual view; C2, right tooth row buccal view. Digital reconstructions from micro CT scans. Letters in grey color indicate tooth positions represented by empty alveoli of lost teeth. Arrows in bold indicate anterior direction. All scale bars equal 1 mm. [Intended for page width 183 mm]

182x187mm (300 x 300 DPI)

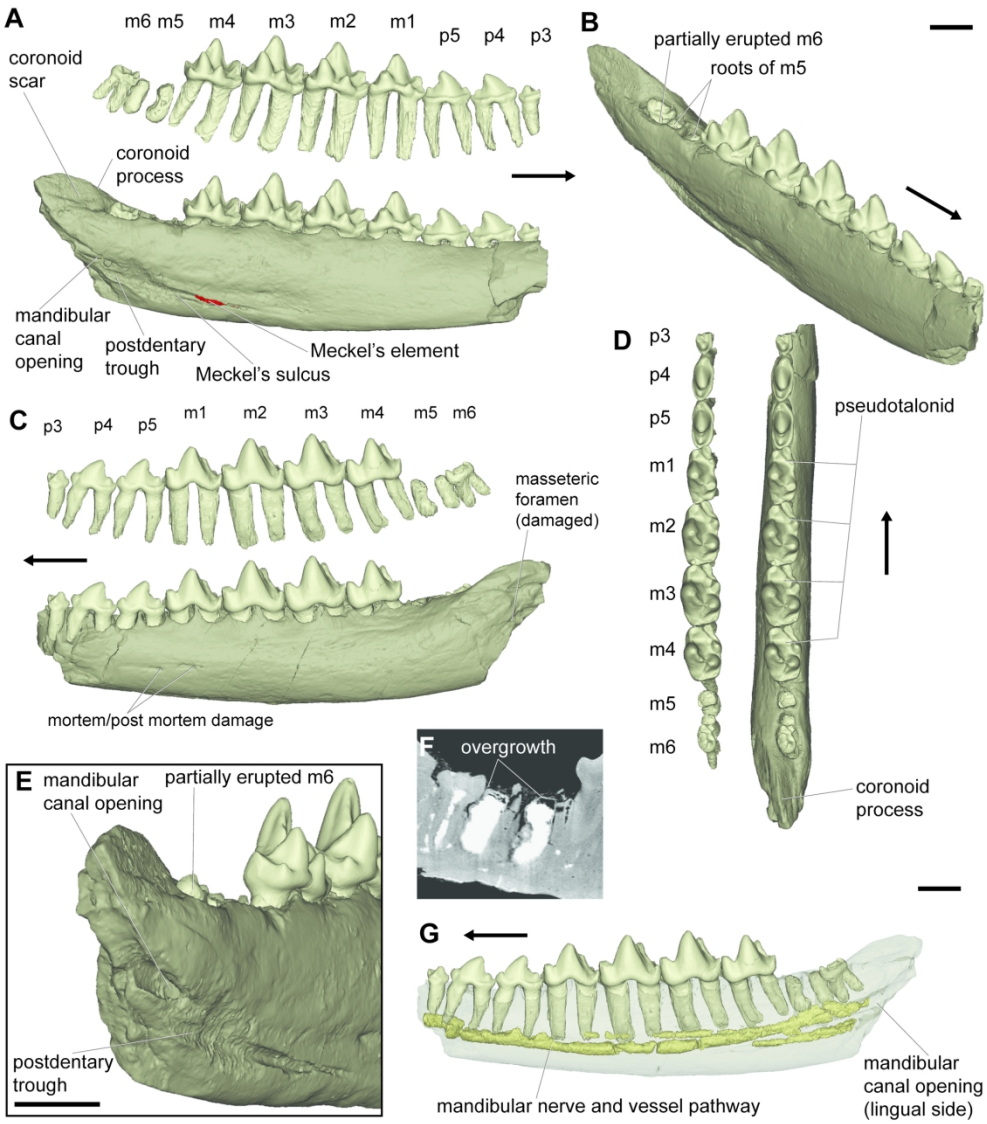

FIGURE 3. *Borealestes serendipitus* BRSUG 20570 (holotype), partial left dentary. A, lingual; B, anterolingual; C, buccal; D, occlusal views of the dentary and dentition; E, posterolingual view showing the opening for mandibular canal and relationship to postdentary trough; F, micro CT scan slice showing the possible overgrowth of m5 roots suggesting pre-mortem tooth loss; G, buccal view of dentary semi-transparent with segmented mandibular nerve and vessel pathway inside the dentary. Digital reconstructions from micro CT scans. Arrows in bold indicate anterior direction. Scale bar same for A–D and G. All scale bars equal 1 mm. [Intended for page width 183 mm]

182x206mm (300 x 300 DPI)

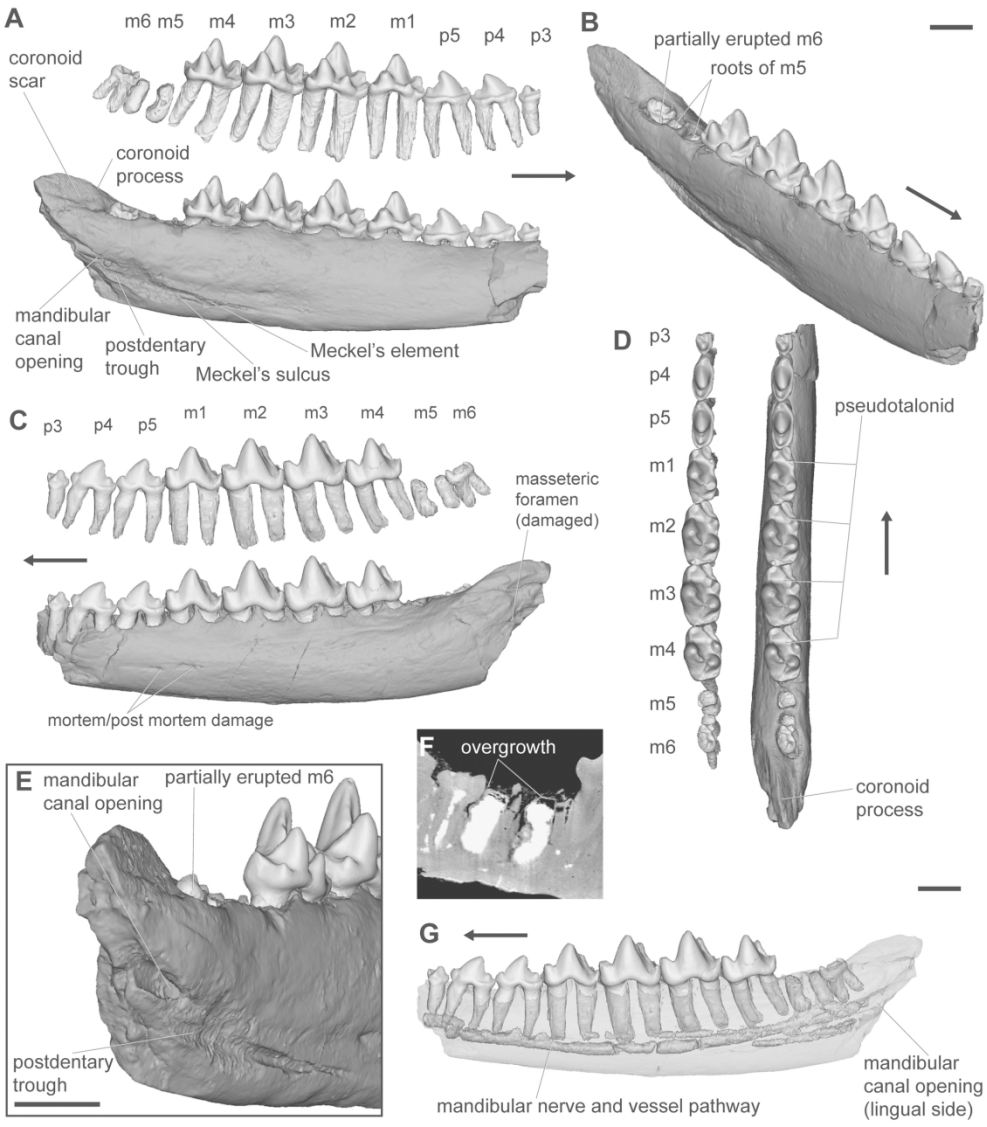

FIGURE 3. *Borealestes serendipitus* BRSUG 20570 (holotype), partial left dentary. A, lingual; B, anterolingual; C, buccal; D, occlusal views of the dentary and dentition; E, posterolingual view showing the opening for mandibular canal and relationship to postdentary trough; F, micro CT scan slice showing the possible overgrowth of m5 roots suggesting pre-mortem tooth loss; G, buccal view of dentary semi-transparent with segmented mandibular nerve and vessel pathway inside the dentary. Digital reconstructions from micro CT scans. Arrows in bold indicate anterior direction. Scale bar same for A–D and G. All scale bars equal 1 mm. [Intended for page width 183 mm]

182x206mm (300 x 300 DPI)

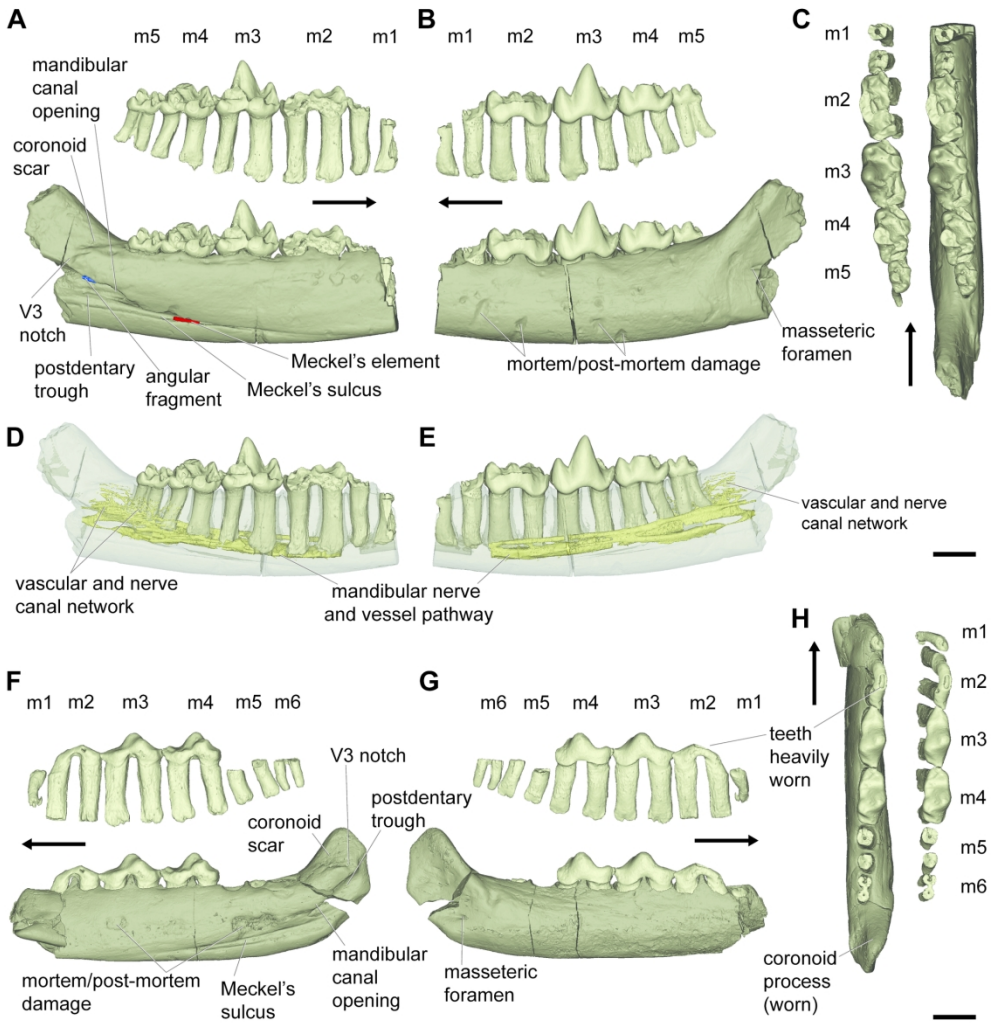

FIGURE 4. *Borealestes serendipitus* BRSUG 20571 (partial left dentary), and BRSUG 29007 (partial right dentary). A, lingual; B, buccal; C, occlusal views of the dentary and dentition of BRSUG 20571. D, lingual; and E, buccal views of the dentary semi-transparent with segmented mandibular nerve and vessel pathway inside the dentary of BRSUG 20571. F, lingual; G, buccal; and H, occlusal views of the dentary and dentition BRSUG 29007. Digital reconstructions from micro CT scans. Arrows in bold indicate anterior direction. Same scale throughout. All scale bars equal 1 mm. [Intended for page width 183 mm]

182x187mm (300 x 300 DPI)

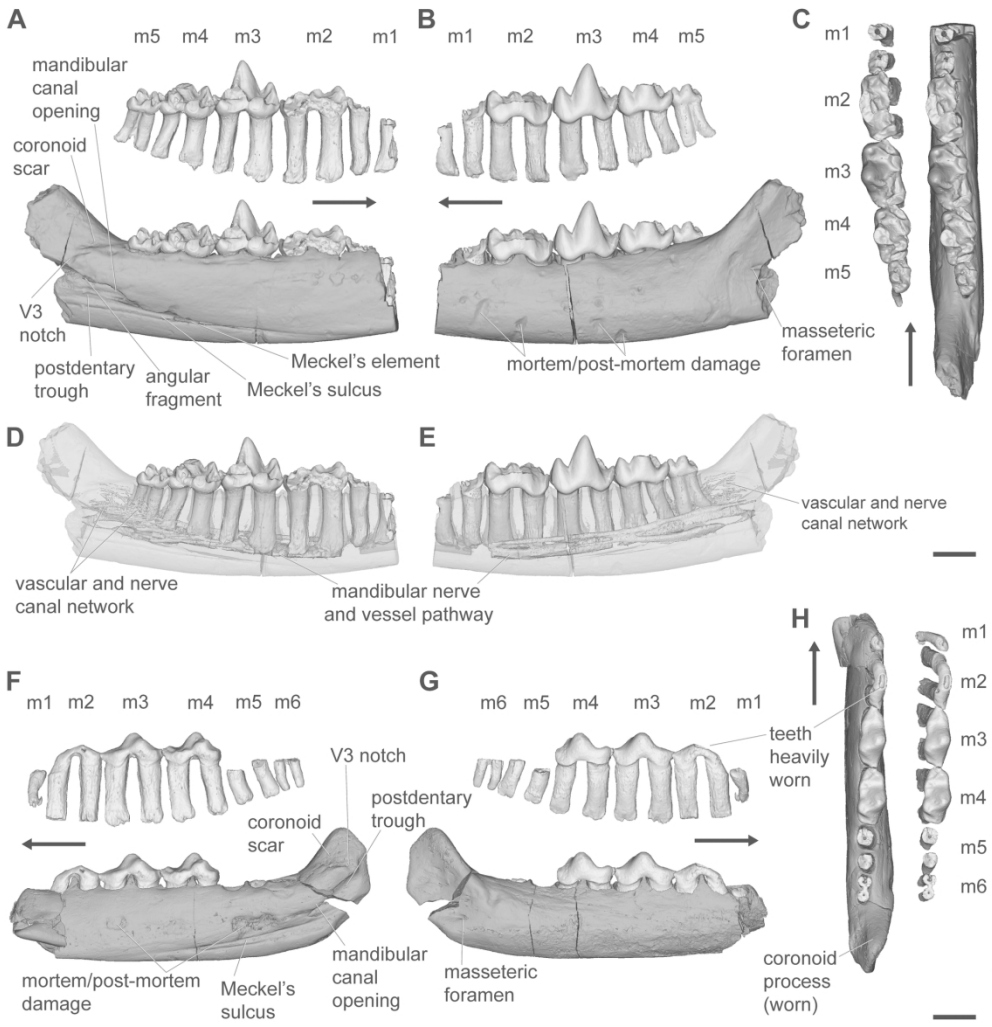

FIGURE 4. *Borealestes serendipitus* BRSUG 20571 (partial left dentary), and BRSUG 29007 (partial right dentary). A, lingual; B, buccal; C, occlusal views of the dentary and dentition of BRSUG 20571. D, lingual; and E, buccal views of the dentary semi-transparent with segmented mandibular nerve and vessel pathway inside the dentary of BRSUG 20571. F, lingual; G, buccal; and H, occlusal views of the dentary and dentition BRSUG 29007. Digital reconstructions from micro CT scans. Arrows in bold indicate anterior direction. Same scale throughout. All scale bars equal 1 mm. [Intended for page width 183 mm]

182x187mm (300 x 300 DPI)

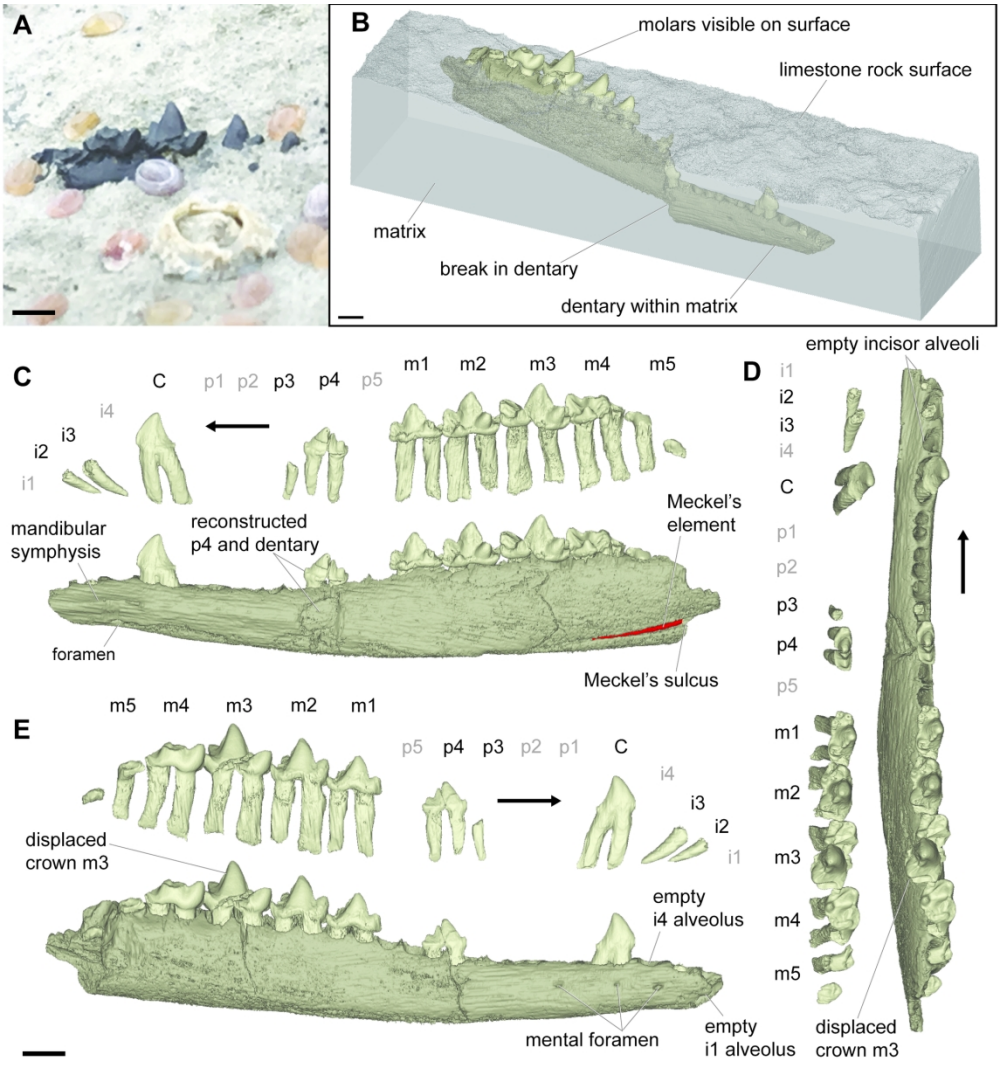

FIGURE 5. *Borealestes serendipitus* NMS G.2018.27.1, partial right dentary. A, the jaw of NMS G.2018.27.1 as found in situ; B, digital reconstruction of dentary in matrix, showing original breakage at p4. Dentary reconstructed from micro CT scans and anterior and posterior portions re-aligned: C, lingual; D, occlusal; and E, buccal view of the dentary and dentition. Letters in grey color indicate tooth positions represented by empty alveoli of lost teeth. Arrows in bold indicate anterior direction. Same scale for C–E. All scale bars equal 1 mm. [Intended for page width 183 mm]

182x196mm (300 x 300 DPI)

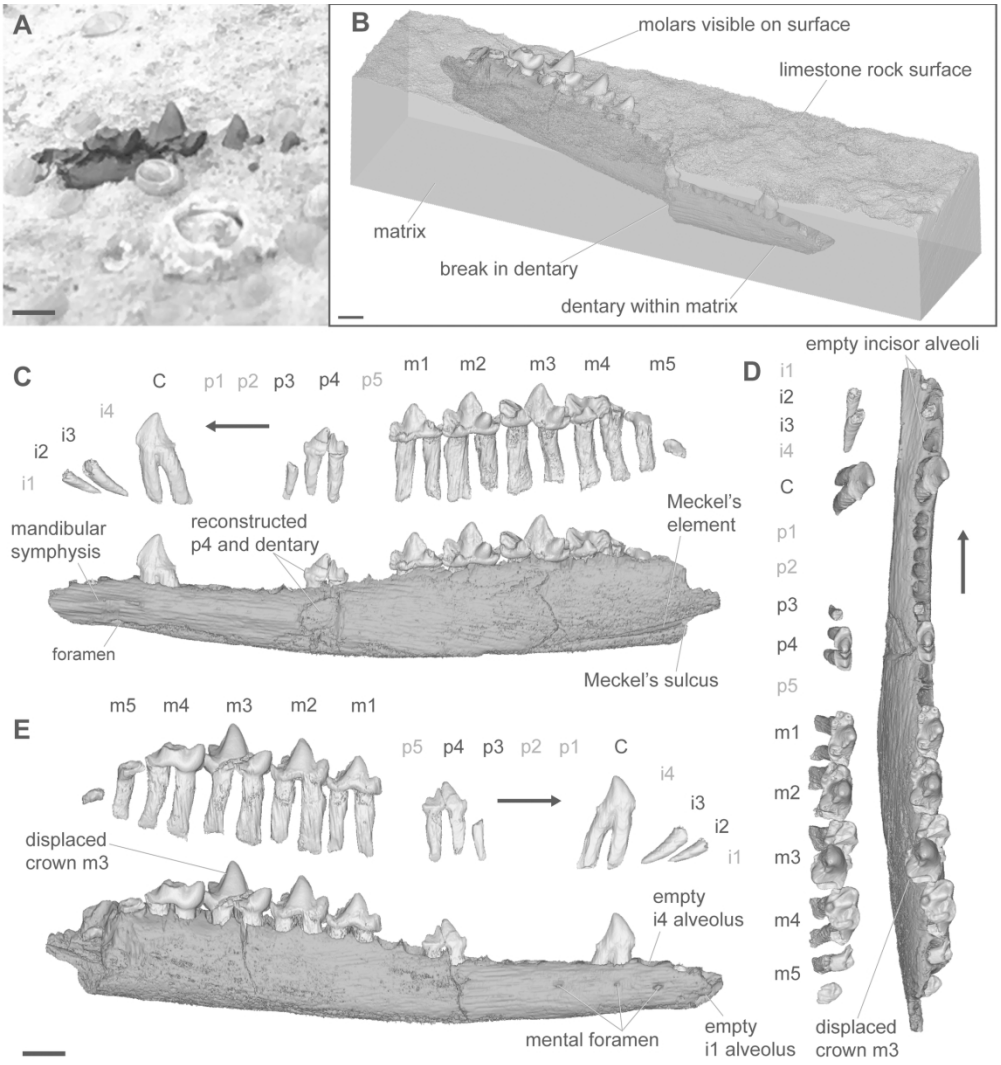

FIGURE 5. *Borealestes serendipitus* NMS G.2018.27.1, partial right dentary. A, the jaw of NMS G.2018.27.1 as found in situ; B, digital reconstruction of dentary in matrix, showing original breakage at p4. Dentary reconstructed from micro CT scans and anterior and posterior portions re-aligned: C, lingual; D, occlusal; and E, buccal view of the dentary and dentition. Letters in grey color indicate tooth positions represented by empty alveoli of lost teeth. Arrows in bold indicate anterior direction. Same scale for C–E. All scale bars equal 1 mm. [Intended for page width 183 mm]

182x196mm (300 x 300 DPI)

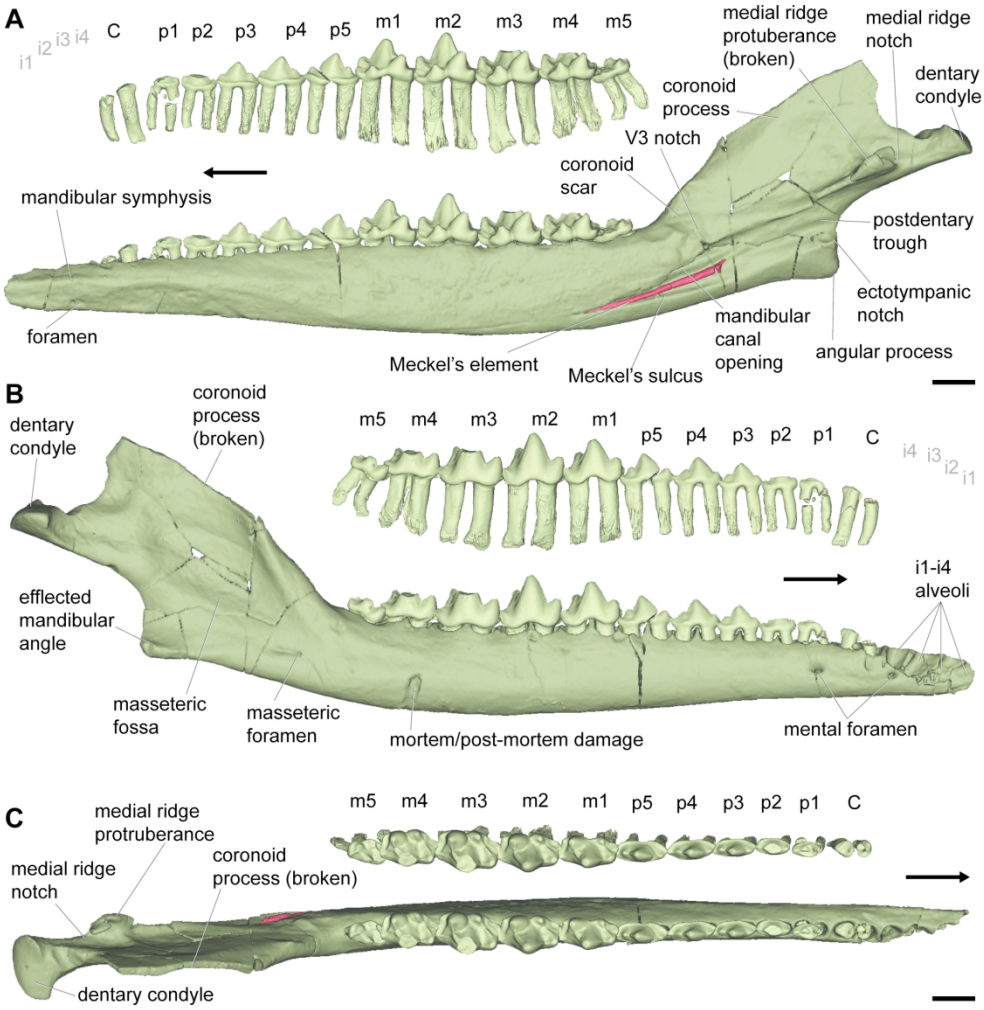

FIGURE 6. *Borealestes serendipitus* NMS G.1992.47.121.3, almost complete right dentary. A, lingual; B, buccal; C, occlusal views of dentary and dentition. Digital reconstructions from micro CT scans. Arrows in bold indicate anterior direction. Scale same throughout. All scale bars equal 1 mm. [Intended for page width 183 mm]

182x186mm (300 x 300 DPI)

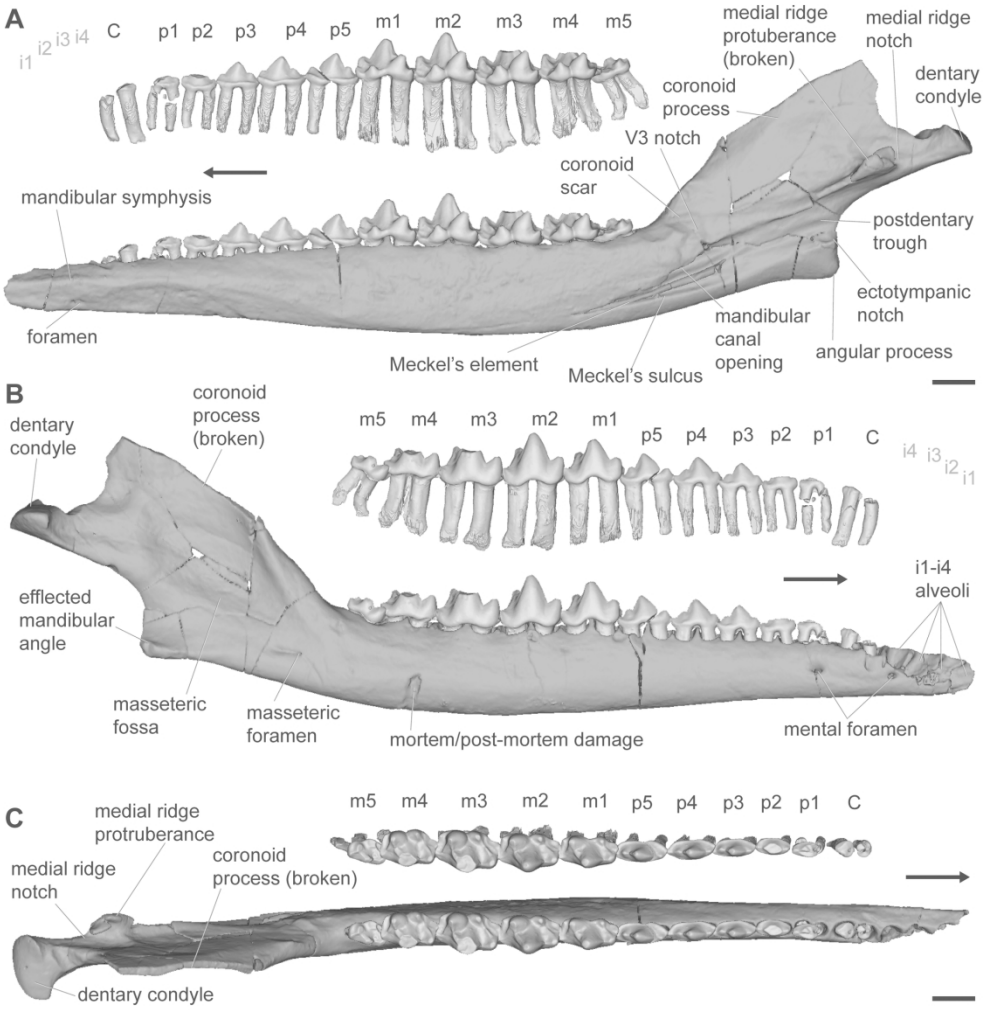

FIGURE 6. *Borealestes serendipitus* NMS G.1992.47.121.3, almost complete right dentary. A, lingual; B, buccal; C, occlusal views of dentary and dentition. Digital reconstructions from micro CT scans. Arrows in bold indicate anterior direction. Scale same throughout. All scale bars equal 1 mm. [Intended for page width 183 mm]

182x186mm (300 x 300 DPI)

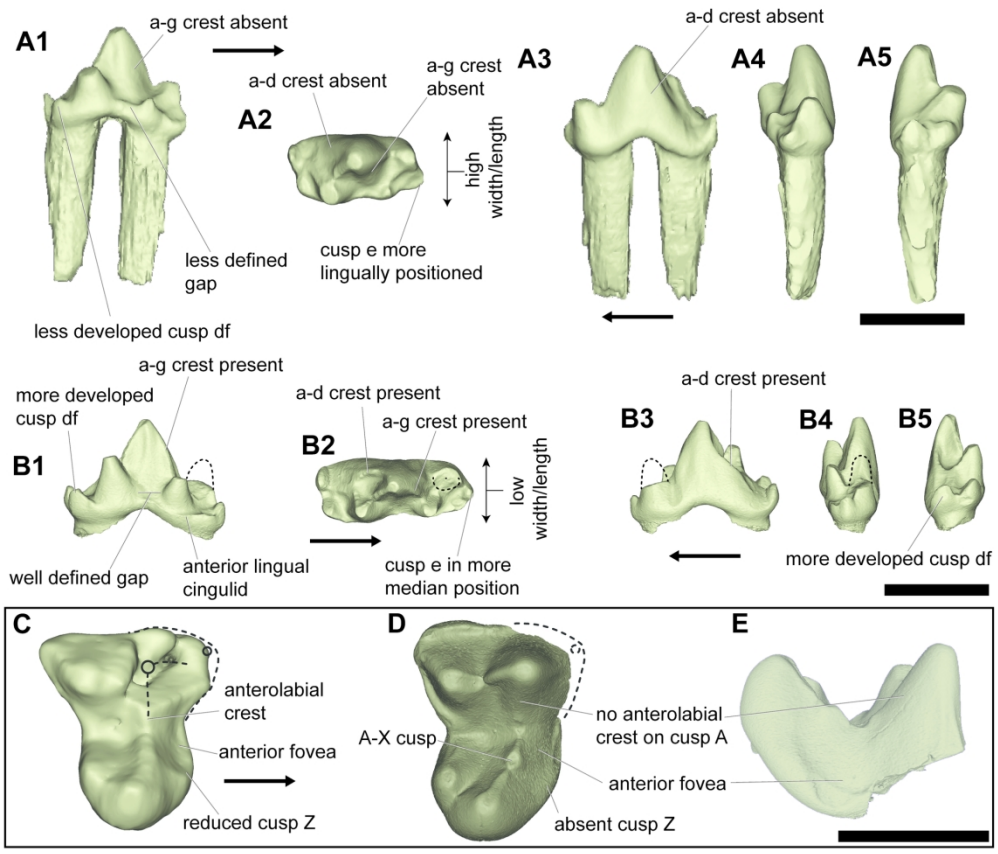

FIGURE 7. Distinguishing characters of *Borealestes serendipitus* and *B. mussettae*. A, and B, lower molar characters. A, *Borealestes serendipitus* based on m1 of holotype BRSUG 20570: A1, lingual; A2, occlusal; A3, buccal; A4, anterior; and A5, posterior views of molar. All B, *B. mussettae* based on holotype NHMUK PV M46495, but crack through cusp a is repaired, and molar mirrored to facilitate comparison: B1, lingual; B2, occlusal; B3, buccal; B4, anterior; and B5, posterior views of molar. C, D and E, distinctive upper molar characters for each species of *Borealestes*: C, M3 of *B. serendipitus*, NMS G.1992.47.121.1; D, *B. mussettae*, NHMUK PV M46871; E, *B. mussettae*, NHMUK PV M46871 anterior view. D and E mirrored to facilitate comparison. Digital reconstructions from micro CT scans. Dotted lines indicate missing portions of tooth. Arrows in bold indicate anterior direction. Same scale for A–B, and same scale for C–E. All scale bars equal 1 mm. [Intended for page width 183 mm]

182x155mm (300 x 300 DPI)

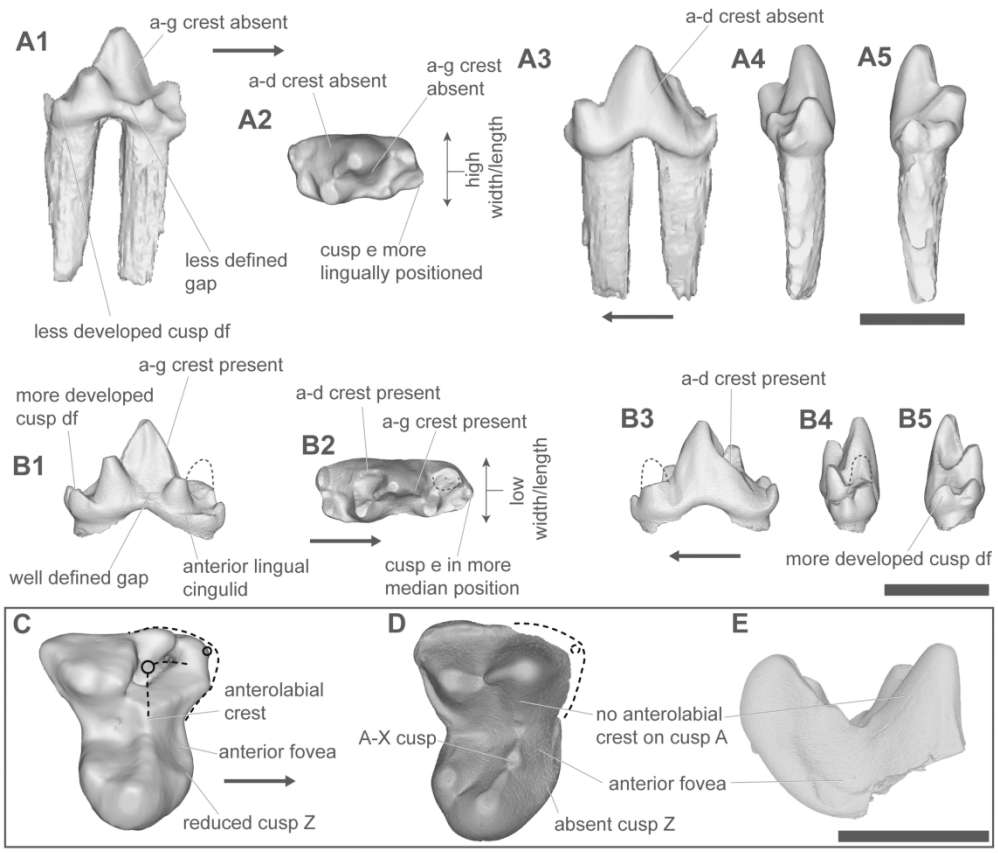

FIGURE 7. Distinguishing characters of *Borealestes serendipitus* and *B. mussettae*. A, and B, lower molar characters. A, *Borealestes serendipitus* based on m1 of holotype BRSUG 20570: A1, lingual; A2, occlusal; A3, buccal; A4, anterior; and A5, posterior views of molar. All B, *B. mussettae* based on holotype NHMUK PV M46495, but crack through cusp a is repaired, and molar mirrored to facilitate comparison: B1, lingual; B2, occlusal; B3, buccal; B4, anterior; and B5, posterior views of molar. C, D and E, distinctive upper molar characters for each species of *Borealestes*: C, M3 of *B. serendipitus*, NMS G.1992.47.121.1; D, *B. mussettae*, NHMUK PV M46871; E, *B. mussettae*, NHMUK PV M46871 anterior view. D and E mirrored to facilitate comparison. Digital reconstructions from micro CT scans. Dotted lines indicate missing portions of tooth. Arrows in bold indicate anterior direction. Same scale for A–B, and same scale for C–E. All scale bars equal 1 mm. [Intended for page width 183 mm]

182x155mm (300 x 300 DPI)

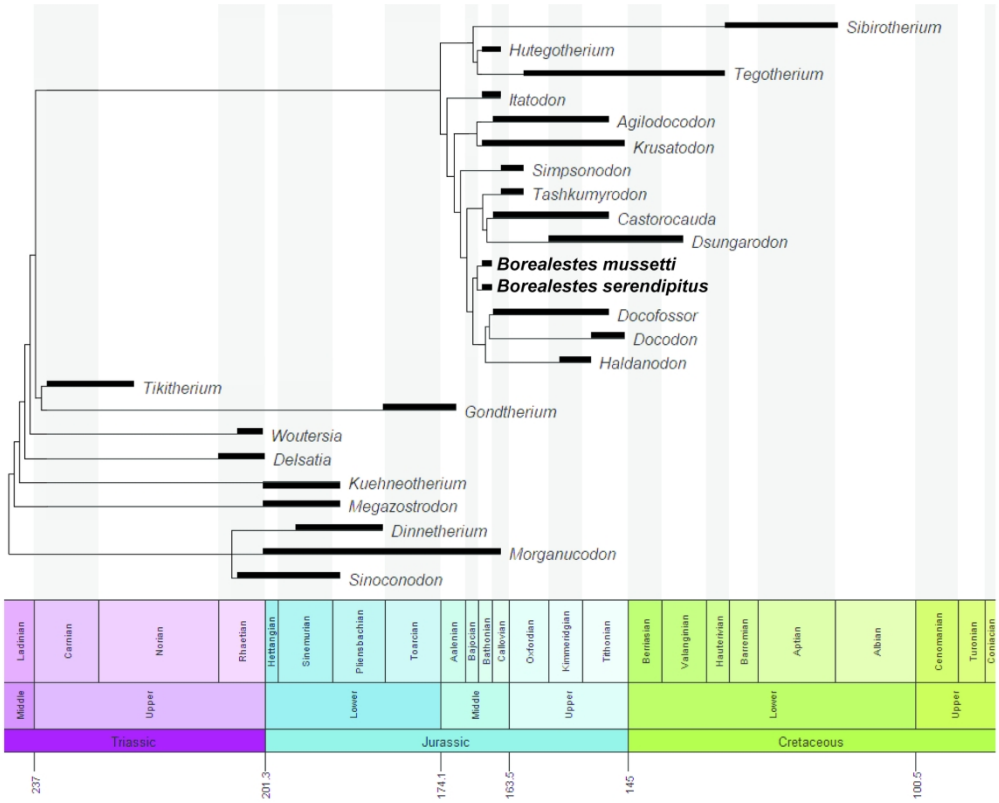

FIGURE 8. Phylogeny of docodonta, with tree-topology based on updated phylogenetic analysis. Results of parsimony branch and bound analysis of docodonts and outgroups, tree of 117 steps. First to last appearances are represented by black box for each taxon (for sources of FAD/LADs see Methods). Nodes uniting taxa do not imply divergence times. [Intended for page width 183 mm]

182x146mm (300 x 300 DPI)

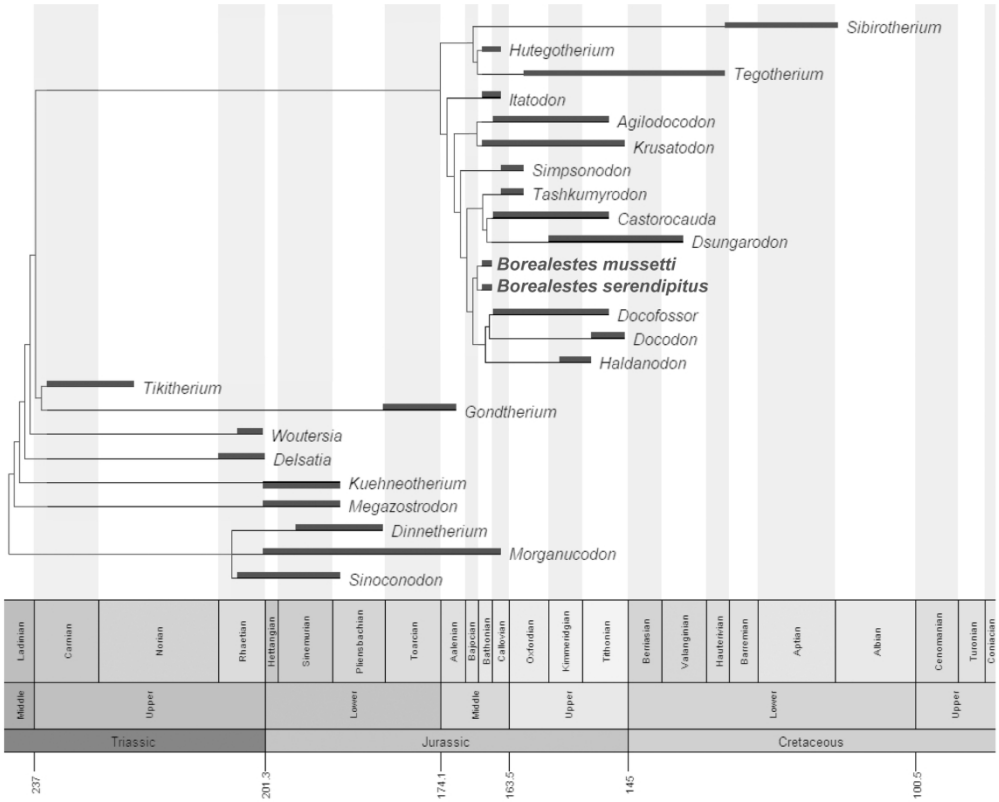

FIGURE 8. Phylogeny of docodonta, with tree-topology based on updated phylogenetic analysis. Results of parsimony branch and bound analysis of docodonts and outgroups, tree of 117 steps. First to last appearances are represented by black box for each taxon (for sources of FAD/LADs see Methods). Nodes uniting taxa do not imply divergence times. [Intended for page width 183 mm]

182x146mm (300 x 300 DPI)

The Journal of Vertebrate Paleontology

The mandible and dentition of *Borealestes serendipitus* (Docodonta) from the Middle Jurassic of Skye, Scotland

ELSA PANCIROLI,[1,2]* ROGER B.J. BENSON,[3] and ZHE-XI LUO[4]*

[1] Natural Science Department, National Museum of Scotland, Edinburgh, Scotland, EH1 1JF, United Kingdom;

[2] School of Geosciences, Grant Institute, University of Edinburgh, Scotland, EH9 3JW, United Kingdom, *elsa.panciroli@ed.ac.uk;

[3] Department of Earth Sciences, University of Oxford, Oxford, England, United Kingdom. roger.benson@earth.ox.ac.uk;

[4] Department of Organismal Biology and Anatomy, The University of Chicago, Chicago, Illinois, U.S.A. zxluo@uchicago.edu

Contents

S1: Docodontan Lower molar terminology

Terminology used in this paper	Butler (1997) & Pfretzschner et al. (2005)	Sigogneau-Russell (2003) & Kielan-Jaworowska et al. (2004)	Luo & Martin (2007)
cusp a	cusp a	main cusp	cusp a
cusp b	cusp b	mesiolabial cusp	cusp b
cusp c	cusp c	distolingual cusp	cusp c
cusp d	cusp d	distolabial talonid cusp	cusp d
cusp e	cusp e	cuspule	cusp e / mesiolingual cingulid cuspule
cusp df	cusp df	lingual talonid cusp	docodont cusp f / distolingual cingulid cuspule
cusp g	cusp g	mesiolingual cusp	cusp g
a-b crest			a-b crest / anterior crest
a-c crest			a-c crest / postero-oblique crest
a-d crest		posteromain crest	
a-g crest		anteromain crest	a-g crest / antero-oblique crest
b-g crest		anterobasal crest	
b-e crest		crescent	
c-d crest			c-d crest / Transtalonid crest
c-f crest		posterior crest	
d-f crest		cingulum	d-f crest / Distal-cingulid crest

S2: Tooth Row Gradients

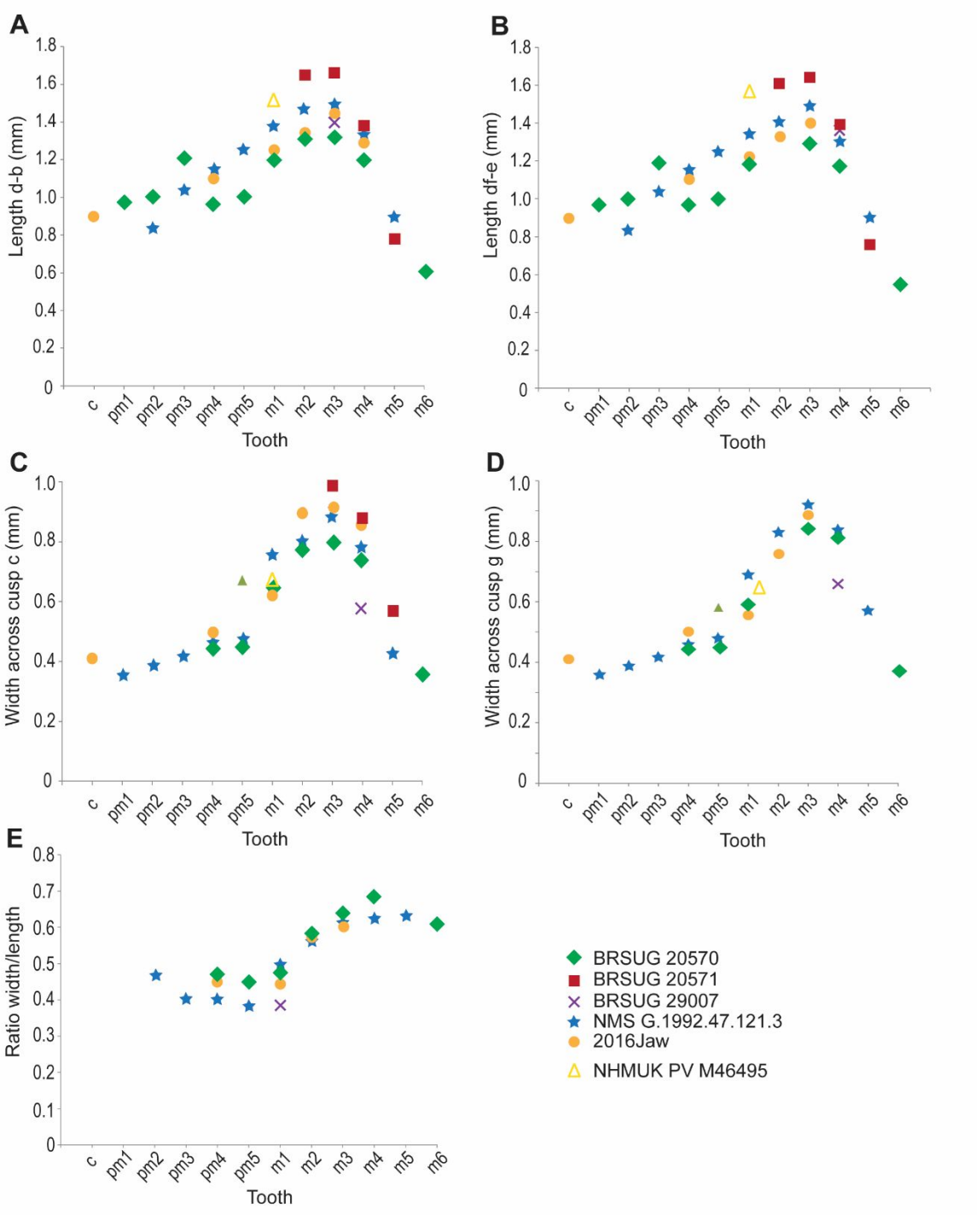

Size gradient and width to length ratio of toothrows of *Borealestes serendipitus* and *B. mussettae* holotype. **A,** length measured from cusp d to b; **B,** length measured from cusp df to e; **C,** width measured across cusp c**; D,** width

measured across cusp g; **E,** the ratio of width divided by length. All measurements in mm. For measurements see Table 1, and for measurement methodology see Figure 1 and text. [Intended for page width 183 mm]

S3: Comparative Figure of *Borealestes serendipitus* Tooth Rows

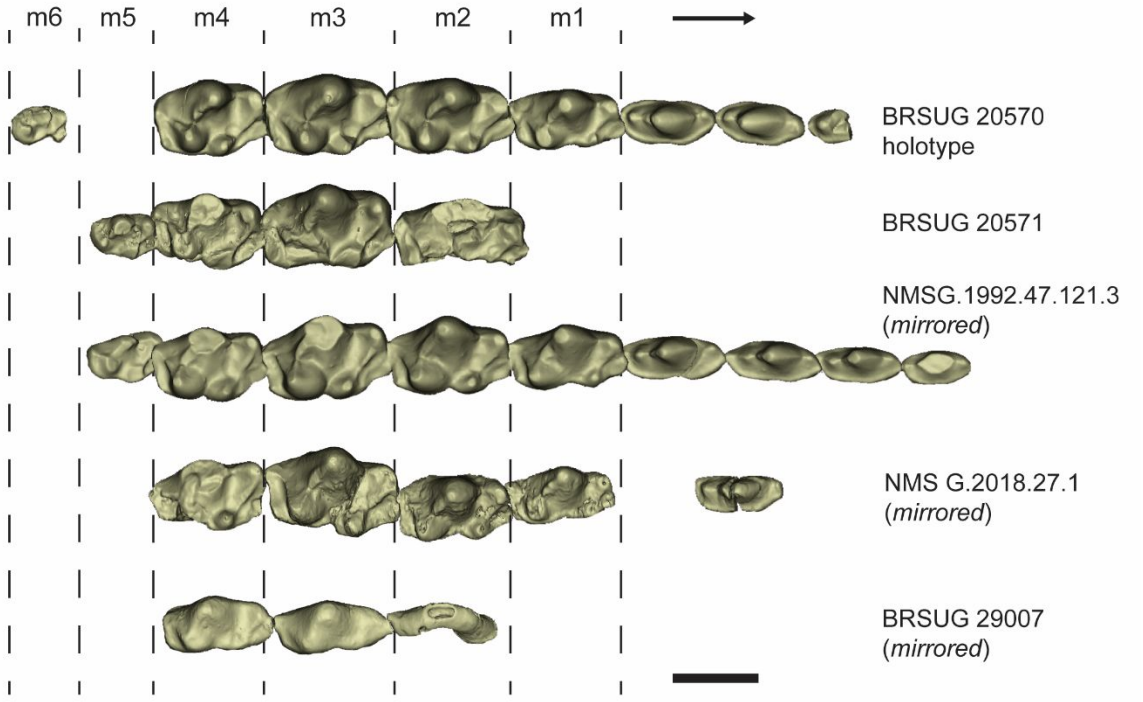

Comparison of multiple specimens of *Borealestes serendipitus.* Lower tooth rows in five specimens of *B. serendipitus*, some mirrored to permit easy comparison with the holotype material. NMS G.2018.27.1 m3 crown was displaced post-mortem and is here placed back to correct position to facilitate comparison. The unusually buccolingually narrow teeth of BRSUG 29007 are caused by post mortem erosion. Same scale throughout. All scale bars equal 1 mm. [Intended for page width 183 mm]

S4: Dentary Condyle of *Borealestes serendipitus* NMS G.1992.47.121.3

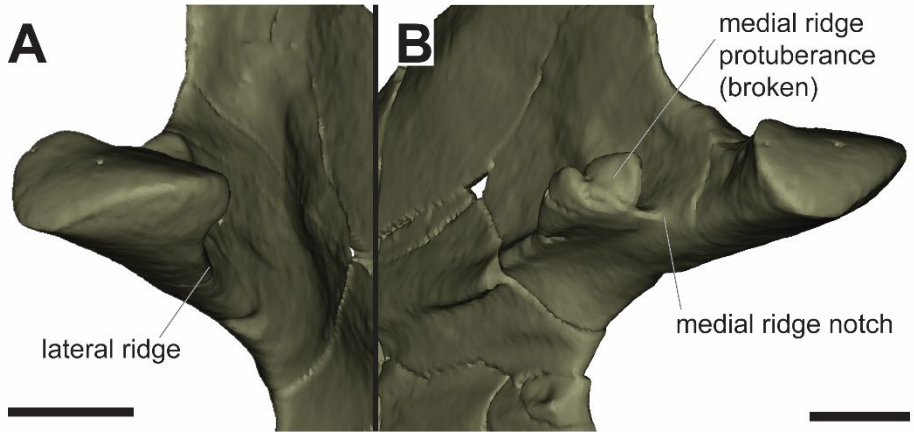

The dentary condyle of specimen NMS G.1992.47.121.3, *Borealestes serendipitus*, showing **A**, the spindle-shaped condyle, and ***B***, the broken and displaced flange of the medial protuberance.

S5: Notes on *Borealestes* Species

Specimens were re-examined in light of refined diagnosis for both species of the genus *Borealestes*. Justification for identifications given (see main text for details of diagnoses).

NHM PV specimen	*B. serendipitus*	*B. mussettae*	Docodonta	Notes on identification
M.44301	yes			The c and g cusp close together, no a-d or a-g crest.
M.46039	yes			Very worn, but lacks a-g or a-d crest.
M.46058	yes			Lacks a-d crest.
M.46116	uncertain			Heavily worn, ID uncertain but probably *B. serendipitus.*
M.46316	yes			No cusp on the A-X crest.
M.46396	yes			Strong A-X crest as expected for *B. serendipitus*.
M.46400			yes	The tooth doesn't match morphology of molar of *Borealestes*: too

				anteroposteriorly elongated, with large cingulid cusps B and C. Not *Borealestes*.
M.46445			yes	Cusp Y too large, indent too deep, A-X crest too distinct. This incomplete tooth is probably a labial wing of *Krusatodon* right upper molar.
M.46521	yes			No a-g and a-d crest (not even on cusp d). Posterior cingulid cuspules almost non-existent.
M.46549	yes			No a-d crest.
M.46580		yes		Cuspule on the A-X crest, and distinct cusp Y. No cusp Z.
M.46607			yes	Resembles M46400, but does not resemble *B. serendipitus.*
M.46610	yes			No a-g, no a-d, has all diagnostic morphology of *B. serendipitus*.
M.46632	probably			Very worn, but nothing contradicts an ID as *B. serendipitus.*
M.46728	probably			Not any major diagnostic features, but nothing contradicts an ID as *B. serendipitus.*
M.46791	yes			No a-g, or a-d. Has diagnostic morphology of lower molar *B. serendipitus*, with very small cusp g far from cusp c, indicating an m1.
M.46841	yes			No a-d or a-g crest.
M.46869	yes			Anteriorly very worn, no a-d crest or a-g crest.
M46246	no	unlikely	Probably	This was labelled as *Borealestes* cf. *mussettae,* but it almost certainly neither as it has none of the diagnostic features.
M46845	likely			Referred to 'Docodonta', but likely *B. serendipitus*, indicated by a very weak a-g crest.
M46842	yes			Referred to 'Docodonta', but likely *B. serendipitus*, no a-g crest.
M. 46001		yes		Has strong a-g crest and a-d crest.

M. 46066		yes		Has a-g crest.
M.46224		yes		Has a-g crest and well defined pseudotalonid by a-g and b-g crests.
M.46239		yes		Has a-g, a-c, and a-b crests. Longer length/width ratio.
M.46319		yes		Worn, but has a-d crest and wide space between cusps c and g.
M.46389	yes			No a-g crest, the tooth is bucco-labially wide.
M.46394		yes		The A-X crest weak to non-existent.
M.46399	yes			Strong c-d cusp and no a-d cusp.
M.46401	yes			No a-d crest.
M.46404	no	probably not	yes	Very fragmentary; the preserved part is probably the labial wing of upper molar. Could be *Krusatodon,* certainly not *B. serendipitus* as there is a cusp on the A-X crest - if it *is* an A-X crest.
M.46448		yes		Cusp on A-X crest and a more distinct cusp Y than in *B. serendipitus*.
M.46495		HOLOTYPE		See main text and figures.
M.46588	yes			No a-d crest, buccolingually wide.
M.46809		yes		Has a-g crest.
M.46835		yes		Worn and enamel broken, but seems to show an a-g crest; c and g cusps far apart, and the overall morphology buccolingually narrow.
M.46836		yes		Has strong a-g crest and a-d crest.
M.46871		yes		See main text and figures.
J.79446			yes	Has an a-g crest, not a tooth of *B. serendipitus*; cusps c and g close together and strong a-g and a-c crests, but not matching *B. mussettae.* Likely an anterior lower molar of *Krusatodon* or *Simpsonodon*.
J.79474	yes			No a-g crest, but all other features are diagnostic of *B. serendipitus*.
J.79475	yes			No a-g or a-d crest
J.79497			yes	Has an a-g crest, wrinkled enamel on posterior of molar, probably a tooth of *Simpsonodon*.
J.79498	maybe	maybe	maybe	Probably a premolar, not diagnostic features for ID.
J.79514			yes	Strong a-g crest and a-d crest, cusp a conical, very tall and pointed, strong lingual cingulid, large cusp b. Doesn't match *Borealestes*. No wrinkled enamel. Cusps c and g missing, but resembles *Krusatodon*.

S6: Data Matrix Used in this Analysis

```
#NEXUS
Begin data;
Dimensions ntax=25 nchar=47;
Format datatype=standard symbols="01234" gap=-;
Matrix
Sinoconodon   00010000000000000?00???0000?000?0000000?00000 00
Morganucodon 000000000000000010000??0000?00000000000?1000000
Dinnetherium  100100000000000010000??0000?00000000000?1000000
Megazostrodon 100000000000000010000??0000?00000001000?2000000
Kuehneotherium 1001?000000000000?00???0000?00020001000?2010000
Delsatia ??????????????1021000??0000?00000001000?20100??
Woutersia ?????10000101010210000??0000?00000001000?201000?
Gondtherium ?????110000020???????????0?????????????????????
Tikitherium ?????110000021???????????0??????????????????????1?
Haldanodon2111111112112110313111001110211111101111 4012011
Docodon 2111111112112111313111101110210210100111 4012011
Docofossor 211111111211211131311100101021021110?1114012011
Dsungarodon ?????111110121103112100110102101010012101111111
BorealestesS 11101111110121103011120010 1?1112111011103011111
BorealestesMUp ?????110?10121103022010010201111111101110?1101??
Tashkumyrodon ??????????????103?3211101020?01101101211111111??
Castorocauda  211?1?????????10311210101020110201001210101 11?1
Itatodon  ???11?????????10413201?0102011010110121030111?1
Simpsonodon ????111111011010411 21?10112011110110121030111 1?
Krusatodon ?????11?0101111031221201102110110110121030111 1?
Agilodocodon  2111111101 011110412212111121101101101210301 1111
Tegotherium ???111111011110412200111020000101102210311111?
Hutegotherium ??111111011110412200111020000101102210311111?
Sibirotherium  ???111111011110312200101020000101102210311 1111
;
End;
```

S6: Characters Scores for *B. serendipitus*

Characters were scored using the Meng et al (2015) matrix – see S5 for full character list. The following scores were added or changed.

Additional characters added:

48: Presence of an anterior fovea on the upper molars: (0) absent, (1) present and positioned at mid-line constriction of upper molar, (2) present and lingually offset from the midline of the upper molar.

This character is absent in all docodonts except *Docodon* (2) and *Borealestes* (1).

1-5: characters can now be scored thanks to new material

8 and 9: defined as mesio-lingual and mesio-labial crests (Meng et al 2015), but meaning anterolingual and anterolabial. Supplementary of Meng et al (2015) gave character states for character 9 as (0) and (2), this has been amended to (0) and (1).

18: cusp c re-scored, from (1) sub-equal to cusp g, to (0) much larger than cusp g.

19: the anterior border of the pseudo-talonid was scored as (1) present and bordered by the b-g crest. In Meng et al 2015 the score for this character differed between the character list (2), the matrix table (3), and the Nexus file (1).

20: a-g crest re-scored from (2) raised with v-notch, to (1) present or lower. Although there is no a-g crest on cusp a in *B. serendipitus*, there is a very a small portion of crest variably on cusp g, and so this cannot be scored as absent.

21: the b-g crest has been rescored from (0) absent or weakly developed, to (1) present.

27: the a-d crest was re-scored from (2) connected by a crest with a v-notch, to (1) incomplete. This is because the a-d crest is only present on the d cusp, where is runs labially below the a cusp, and is not present on the a cusp.

28: the alignment of the a-d cusp was re-scored from (0) present and straight to (?) not applicable, because it is not present on cusp a.

32: The mesio-lingual cingulid from cusp e was re-scored from (1) extending posteriorly below cusp g to (2) absent or limited to mesial part of the tooth. This cingulid does not extend below cusp g in *B. serendipitus*.

42: the placement of cusp e was re-scored from (1) cusp e labially shifted to (0) lingual position.

44: the degree of triangulation of cusps g-a-c was re-scored from (0) >80 degrees to (1) < 80 degrees.

47: the number of canine roots was scored in the matrix of Meng et al 2015 as (1), but listed in their character descriptions as (?). We can confirm it is (1).

S4: Characters scores for *B. mussettae*

Characters were scored using the Meng et al (2015) matrix – see S5 for full character list. The following scores were added or changed.

1 to 5: the dentary is not yet known for *B. mussettae*.

8: the transverse anterio lingual and anterolablial crest was scored as (0) absent, unlike *B. serendipitus*.

9: the transverse anterio lingual and anterolablial crest in the posterior molar was scored as (?) unknown, as we believe only the anterior upper molars are known for *B. mussettae*.

19: the anterior border of the pseudo-talonid was scored as (2) present and bordered by the b-e crest, unlike in *B.serendipitus*. This is because of the weaker b-g crest in *B. mussettae* and the subsequent slight shift in the position of the pseudotalonid.

20: unlike *B. serendipitus*, *B. mussettae* has (1) a raised a-g crest and it has a v-notch.

21: the b-g crest was scored (0) absent or weakly developed because it is poorly developed compared to *B. serendipitus*.

22: the c-d crest was scored as present with the c-d crest being straight, unlike the angle in *B. serendipitus*.

27: the a-d crest is (2) present and connected with a v-notch in *B. mussettae*.

32: The mesio-lingual cingulid from cusp e was scored as (1) extending posteriorly below cusp g, in contrast to *B. serendipitus*.

41: this was scored as (?) because the interlocking between lower molars is not yet known for *B. mussettae*.

42: the placement of cusp e was scored as (1) cusp e labially shifted to for this species, in contrast to *B. serendipitus*.

44: the degree of triangulation of cusps g-a-c was scored as (0) >80 degrees, in contrast to *B. serendipitus*.

46 and 47: the number of roots in the canine and upper molars is not yet known for *B. mussettae*.

S7: Cross-reference and Scoring of Other Taxa in Meng et al (2015) Matrix

Character lists in Meng et al (2015) differed between the NEXUS file, the matrix table provided for score verification, and the example scores in the character list. We compared these data matrices, and where scores differed we scored those characters based on our own observations of specimens, predominantly from the literature.

Sinoconodon
21: crest b-g (?) not applicable
32: changed to (?) not applicable

Morganucodon
3: changed to (0) facing medially

Dinnetherium
3: changed to parallel to ventral margin (through observation of specimen MCZ 20870)

Megazostrodon
3: changed to (0) convergent to ventral margin

Kuehneotherium
21: changed to (?) not applicable
32: changed to (2) limited to the mesial part of the tooth

Woutersia
9: changed to (0) absent

Gondtherium
9: changed to (0) absent

Tikitherium
9: changed to (0) absent
14: changed to (1) present

Haldanodon
17: changed to (3) distinctive and anteriorly positioned
34: changed to (1)

Docodon
17: changed to (3)

34: changed to (0)
37: changed to (0)

Docofossor
17: changed to (3)
31: changed to (0)

Dsungarodon
1 and 2: changed to (?), although *Acuodulodon* and *Dsungarodon* have been suggested to be synonymous by Martin et al 2010, we consider the material too poorly preserved to be certain, and the synonymisation relies too heavily on premolar characters, which are similar among some docodontans genera (and therefore may be similar in this case). We therefore choose not to use this interpretation for this analysis.
17: changed to (3)
31: changed to (0)

Borealestes
See S1 and S2 for new scores

Tashkumyrodon
17: changed to (3)
19: changed to (3)

Castorocauda
17: changed to (3)
19: changed to (1)

Itatodon
17: changed to (4)
19: changed to (3)
And extra character removed from end

Simpsonodon
17: changed to (4)
19: changed to (1)
22: changed to (?) not applicable due to enamel folding
31: changed to (1)
32: changed to (1)

Krusatodon
17: changed to (3)
23: changed to (0)
31: changed to (1)

Agilodocodon

17: changed to (4)
31: changed to (1)

Tegotherium
17: changed to (4)
21: changed to (0)

Hutegotherium
17: changed to (4)
21: changed to (0)

Sibirotherium
21: changed to (0)
23: changed to (0)

S8: PAUP Analysis

```
P A U P *
Version 4.0a (build 163) for 32-bit Microsoft Windows (built on Jul 23 2018 at 17:54:24)
Wed Sep 05 09:30:24 2018

paup> ToNEXUS fromFile='Mengetal2015matrixAMENDED_ALL5.9.18.txt';

Processing of file "F:\Manuscripts\Borealestes dentary\Phylogenetic
analysis\PAUP\Mengetal2015matrixAMENDED_ALL5.9.18.txt" begins...

Data matrix has 24 taxa, 48 characters
Valid character-state symbols: 01234
Missing data identified by '?'
Gaps identified by '-'

Processing of input file "Mengetal2015matrixAMENDED_ALL5.9.18.txt" completed.

Input data matrix:

                 1       2       3       4     4
Taxon          123456789012345678901234567890123456789012345678
-------------------------------------------------------------
Sinoconodon     00010000000000000?00???0000?000?0000000?00000000
Morganucodon    00000000000000000010000??0000?00000000000?10000000
Dinnetherium    10010000000000000010000??0000?00000000000?10000000
Megazostrodon   10000000000000000010000??0000?00000001000?20000000
Kuehneotherium  1001?000000000000?00???0000?00020001000?20100000
Delsatia        ??????????????1021000??0000?00000001000?20100??0
```

```
Woutersia      ?????10000101010210 00??0000?00000001000?201000?0
Gondtherium    ?????110000020???????????0?????????????????????0
Tikitherium    ?????110000021???????????0?????????????????????1?0
Haldanodon     21111111121121103131110011102111111011114012011 0
Docodon        211111111211211131311110111021021010011140120112
Docofossor     21111111121121113131110010102102111 0?11140120110
Dsungarodon    ?????111110121103112100110102101010012101111111 0
BorealestesS   11101111110121103011120010 1?11211101110300111111
BorealestesMUp ?????110?10121103022010010201111111011 0?1101??1
Tashkumyrodon  ????????????????103?3211101020?01101101211111111??0
Castorocauda   211?1?????????10311210101020110201001210101 11?10
Itatodon       ???11?????????10413201?01020110101101210301 11?10
Simpsonodon    ????111111011010411 21?10112011110110121030111 1?0
Krusatodon     ?????11?01011110312212011021101101101210301111?0
Agilodocodon   21111111010111104122121111211011011012103011111 0
Tegotherium    ???111111011110412200111020000101102210311111?0
Hutegotherium  ???1111111011110412200111020000101102210311111?0
Sibirotherium  ???11111110111103122001010200001011022103111111 0

paup> BandB mulTrees=no;

Branch-and-bound search settings:
  Optimality criterion = parsimony
    Character-status summary:
      Of 48 total characters:
        All characters are of type 'unord'
        All characters have equal weight
        All characters are parsimony-informative
    Gaps are treated as "missing"
  Initial upper bound: unknown (compute heuristically)
  Addition sequence: furthest
  Initial 'Maxtrees' setting = 100
  Branches collapsed (creating polytomies) if maximum branch length is zero
  'MulTrees' option not in effect; only 1 tree will be saved
  No topological constraints in effect
  Trees are unrooted

Maxtrees reset to 200

Branch-and-bound search completed:
  Score of best tree found = 117
  Number of trees retained = 1
  Time used = 00:03:09 (CPU time = 00:02:45.5)
```

paup> ShowTrees / tOrder=right;

Note: No outgroup has been defined; tree is (arbitrarily) rooted at first taxon.

Tree 1 (rooted using default outgroup)

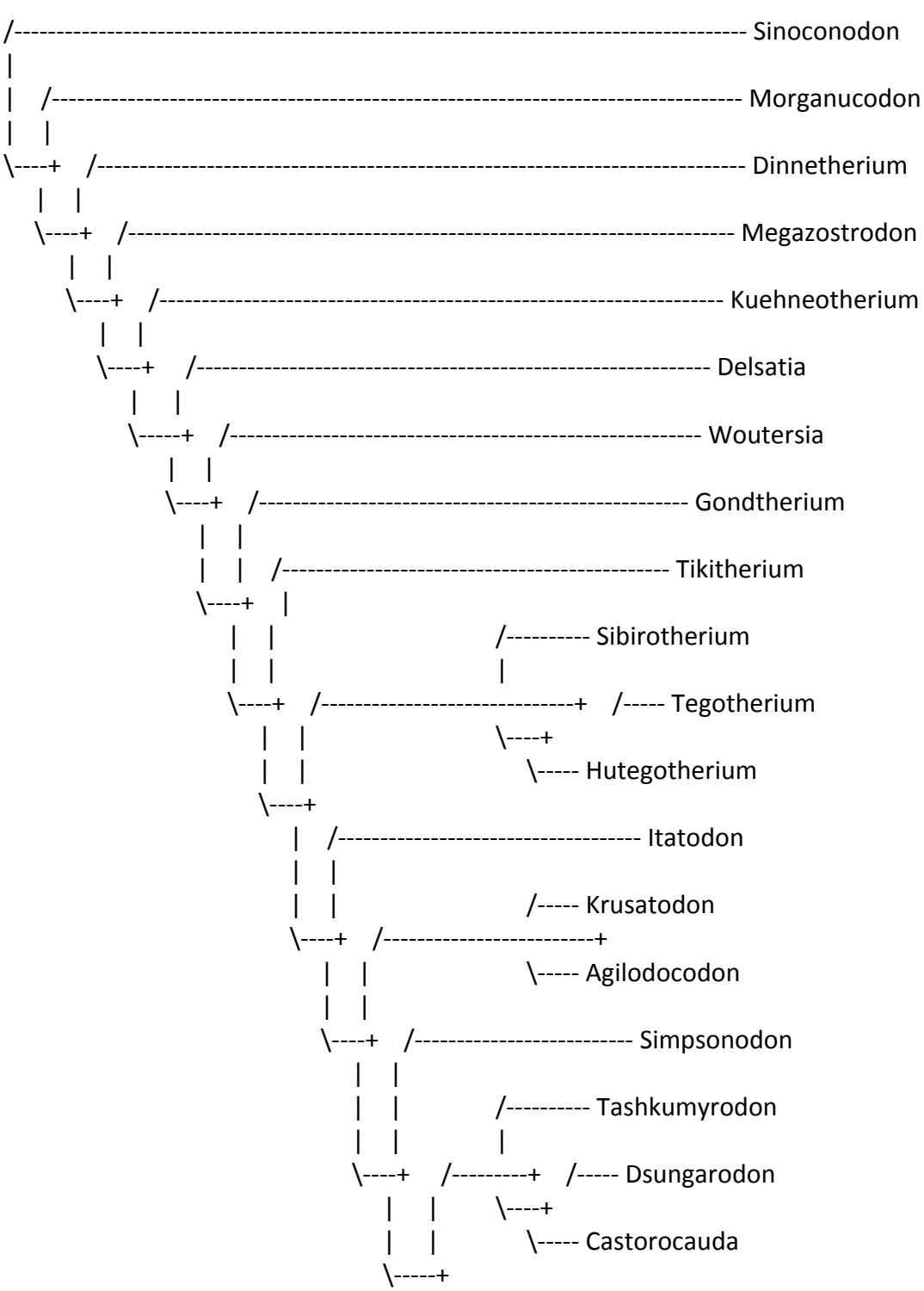

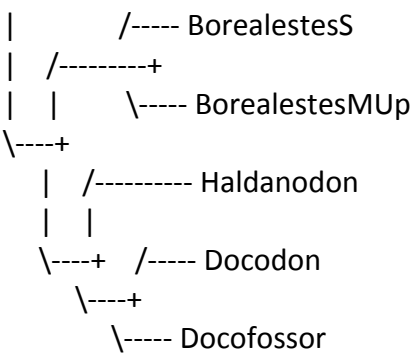


```
paup> DescribeTrees / xout=internal apoList;

Tree description:

  Unrooted tree(s) rooted using outgroup method

  Note: No outgroup has been defined; tree is (arbitrarily) rooted at first taxon.
  Optimality criterion = parsimony
    Character-status summary:
      Of 48 total characters:
        All characters are of type 'unord'
        All characters have equal weight
        All characters are parsimony-informative
    Gaps are treated as "missing"
    Character-state optimization: Accelerated transformation (ACCTRAN)

Tree 1 (rooted using default outgroup)

Reconstructed states for internal nodes:

                 1       2       3       4     4
Node         123456789012345678901234567890123456789012345678
------------------------------------------------------------
25           211111111211211131311100111021021110011140120110
26           211111111211211031311100111021111110111140120110
27           111011111101211030111100101011111110111030111111
28           211111111101211031111100101011111110111030111110
29           211111111101211031121010102011010100121011111110
30           211111111101211031121110102011110110121011111110
31           211111111101211031121110102011110110121030111110
32           211111111101111041121110102011110110121030111110
33           211111110101111041221211102110110110121030111110
34           211111111101111041221110102011110110121030111110
35           211111111101111041220110102011010110121030111110
```

36	21111111110111104122001110200001011022103111111 0
37	21111111110111104122001010200001011022103111111 0
38	21111111110111104122001010200001011012103011111 0
39	21111110000021104122001010200001011012103011111 0
40	21111110000020104122001010200001011012103011111 0
41	21111100000010102100001000000000000100002010001 0
42	21111100000010102100001000000000000100002010001 0
43	10011000000000000100001000000000000100002010000 0
44	10010000000000001000001000000000000100002000000 0
45	10010000000000001000001000000000000000001000000 0
46	00010000000000001000001000000000000000001000000 0

Tree length = 117
Consistency index (CI) = 0.5812
Homoplasy index (HI) = 0.4188
Retention index (RI) = 0.8287
Rescaled consistency index (RC) = 0.4816

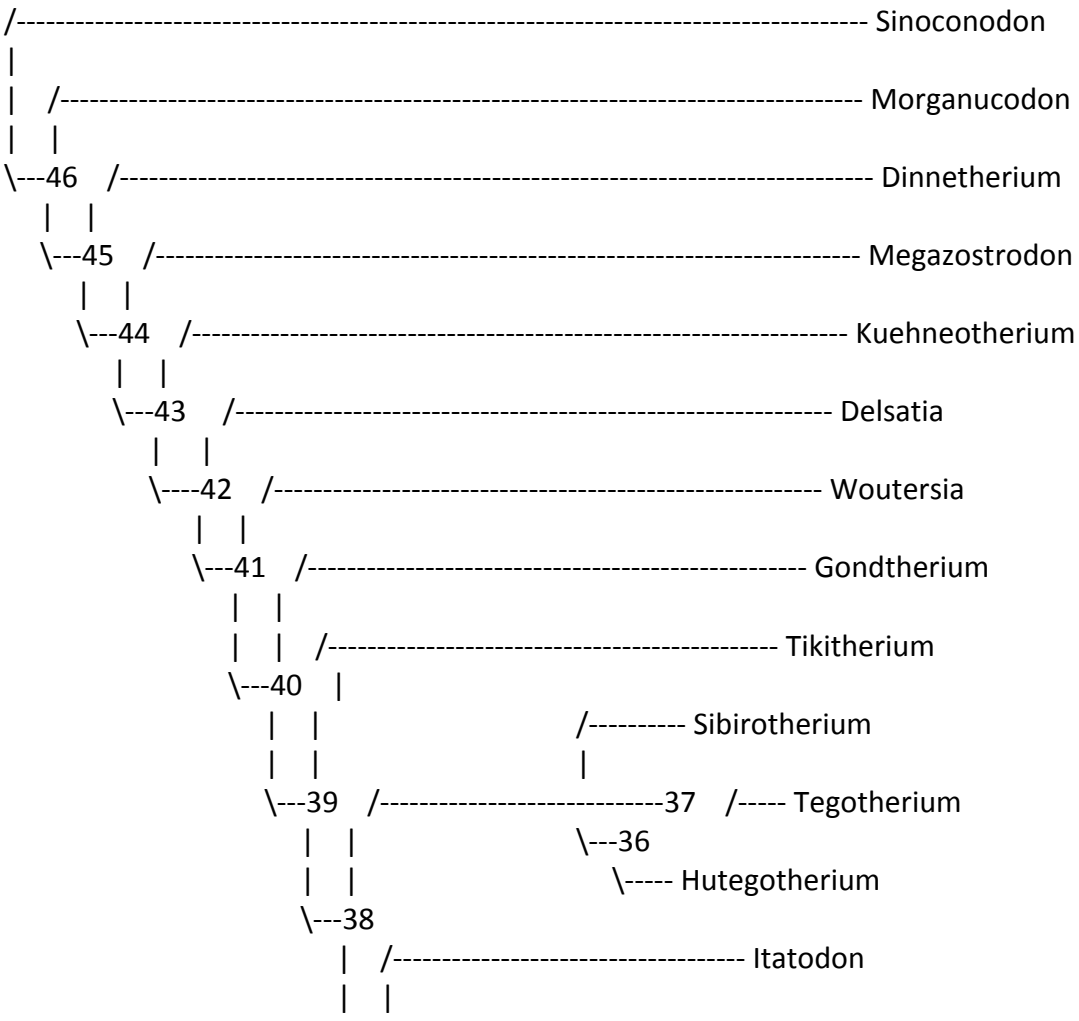

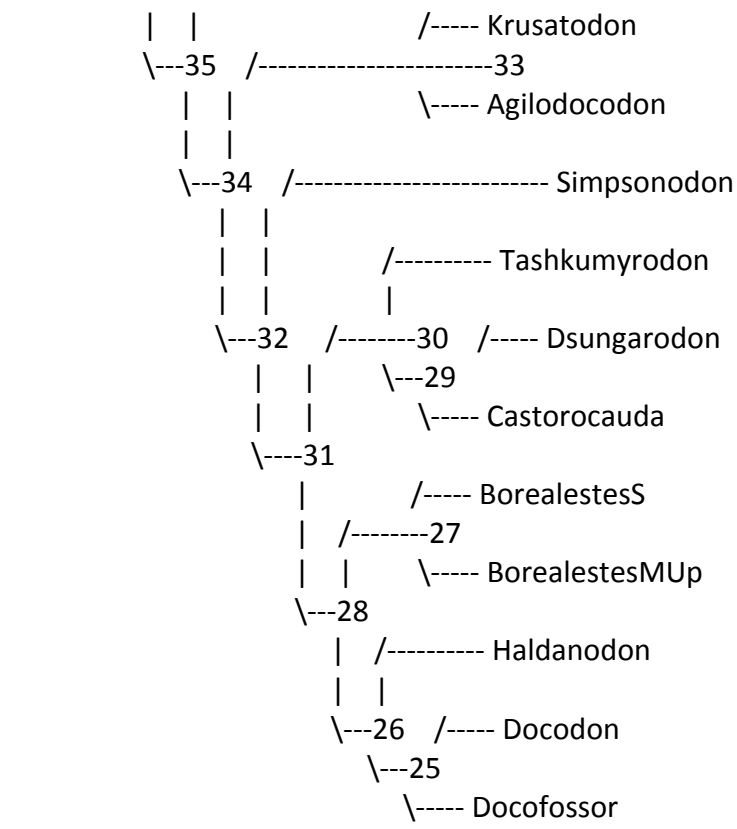

Apomorphy lists:

Branch	Character	Steps	CI	Change
node_46 <-> Sinoconodon	17	1	0.571	1 <=> 0
	41	1	0.800	1 <=> 0
node_46 --> Morganucodon	4	1	0.333	1 ==> 0
node_46 --> node_45	1	1	0.667	0 ==> 1
node_45 --> node_44	36	1	0.500	0 ==> 1
	41	1	0.800	1 ==> 2
node_44 --> Megazostrodon	4	1	0.333	1 ==> 0
node_44 --> node_43	5	1	1.000	0 --> 1
	17	1	0.571	1 --> 0
	18	1	0.500	0 --> 1
	43	1	1.000	0 ==> 1
node_43 --> Kuehneotherium	32	1	0.400	0 ==> 2
node_43 --> node_42	1	1	0.667	1 --> 2
	2	1	1.000	0 --> 1
	3	1	1.000	0 --> 1
	6	1	1.000	0 --> 1
	13	1	0.500	0 --> 1
	15	1	1.000	0 ==> 1

```
                    17          1   0.571  0 --> 2
                    47          1   1.000  0 --> 1
node_41 --> Woutersia     11          1   0.500  0 ==> 1
node_41 --> node_40       7           1   1.000  0 ==> 1
                    13          1   0.500  1 --> 2
                    17          1   0.571  2 --> 4
                    19          1   0.500  0 --> 2
                    20          1   0.667  0 --> 2
                    25          1   1.000  0 --> 1
                    27          1   0.500  0 --> 2
                    32          1   0.400  0 --> 1
                    34          1   0.500  0 --> 1
                    35          1   0.500  0 --> 1
                    36          1   0.500  1 --> 0
                    37          1   0.667  0 --> 1
                    38          1   1.000  0 --> 2
                    39          1   1.000  0 --> 1
                    41          1   0.800  2 --> 3
                    44          1   0.667  0 --> 1
                    45          1   0.500  0 --> 1
                    46          1   1.000  0 --> 1
node_40 --> node_39       14          1   0.500  0 ==> 1
node_39 --> node_38       8           1   0.500  0 ==> 1
                    9           1   0.500  0 --> 1
                    10          1   1.000  0 ==> 1
                    12          1   1.000  0 ==> 1
                    13          1   0.500  2 --> 1
node_38 --> node_35       22          1   0.500  0 --> 1
                    29          1   0.667  0 ==> 1
                    30          1   0.333  0 --> 1
node_35 --> node_34       21          1   0.500  0 ==> 1
                    31          1   0.333  0 ==> 1
node_34 --> node_32       19          1   0.500  2 ==> 1
node_32 --> node_31       13          1   0.500  1 ==> 2
                    17          1   0.571  4 ==> 3
node_31 --> node_28       20          1   0.667  2 --> 1
                    23          1   0.250  1 ==> 0
                    27          1   0.500  2 --> 1
                    33          1   1.000  0 ==> 1
                    38          1   1.000  2 ==> 1
node_28 --> node_26       10          1   1.000  1 ==> 2
                    11          1   0.500  0 ==> 1
                    19          1   0.500  1 ==> 3
                    26          1   0.250  0 --> 1
```

```
                29          1   0.667  1 ==> 2
                40          1   0.500  0 ==> 1
                41          1   0.800  3 ==> 4
                44          1   0.667  1 ==> 2
                45          1   0.500  1 ==> 0
node_26 --> node_25     16          1   1.000  0 ==> 1
                31          1   0.333  1 ==> 0
                32          1   0.400  1 ==> 2
                37          1   0.667  1 --> 0
node_25 --> Docodon     23          1   0.250  0 ==> 1
                34          1   0.500  1 ==> 0
                48          1   1.000  0 ==> 2
node_25 --> Docofossor  26          1   0.250  1 --> 0
node_28 --> node_27     1           1   0.667  2 --> 1
                4           1   0.333  1 --> 0
                18          1   0.500  1 ==> 0
                48          1   1.000  0 ==> 1
node_27 --> BorealestesS    22          1   0.500  1 ==> 2
                32          1   0.400  1 ==> 2
node_27 --> BorealestesMUp 8            1   0.500  1 ==> 0
                19          1   0.500  1 ==> 2
                20          1   0.667  1 --> 2
                21          1   0.500  1 ==> 0
                27          1   0.500  1 --> 2
                42          1   0.250  0 ==> 1
                44          1   0.667  1 ==> 0
node_31 --> node_30     41          1   0.800  3 ==> 1
                42          1   0.250  0 --> 1
node_30 --> node_29     22          1   0.500  1 ==> 0
                31          1   0.333  1 ==> 0
                35          1   0.500  1 ==> 0
node_29 --> Dsungarodon     23          1   0.250  1 ==> 0
                24          1   0.333  0 ==> 1
                27          1   0.500  2 ==> 1
                29          1   0.667  1 ==> 2
node_29 --> Castorocauda    32          1   0.400  1 ==> 2
                42          1   0.250  1 --> 0
node_30 --> Tashkumyrodon   19          1   0.500  1 ==> 3
                30          1   0.333  1 ==> 0
                40          1   0.500  0 ==> 1
node_32 --> Simpsonodon     14          1   0.500  1 ==> 0
                26          1   0.250  0 ==> 1
node_34 --> node_33     9           1   0.500  1 --> 0
                22          1   0.500  1 ==> 2
```

```
                    24          1   0.333  0 ==> 1
                    28          1   1.000  0 ==> 1
                    30          1   0.333  1 --> 0
node_33 --> Krusatodon     17          1   0.571  4 ==> 3
                    23          1   0.250  1 ==> 0
node_33 --> Agilodocodon   26          1   0.250  0 ==> 1
node_35 --> Itatodon       19          1   0.500  2 ==> 3
node_38 --> node_37        37          1   0.667  1 --> 2
                    42          1   0.250  0 ==> 1
node_37 --> node_36        24          1   0.333  0 ==> 1
node_37 --> Sibirotherium  17          1   0.571  4 ==> 3

paup> SaveTrees file='F:\Manuscripts\Borealestes dentary\Phylogenetic
analysis\PAUP\Tree.txt';

1 tree saved to file "F:\Manuscripts\Borealestes dentary\Phylogenetic
analysis\PAUP\Tree.txt"
```

S9: Systematic Character List for Docodontans and Outgroups (see Meng et al 2015)

Mandibular Features

From Meng et al. (2015).

1. Mandible --- Angular process shape:

(0) Pointed angle (two sides of the angular process forming an angle of 90 degrees and higher)

(1) Obtuse angle (two sides of the angular process forming an angle of less than 90 degrees)

(2) Rounded angular process

2. Angular process of the mandible with an efflected ventral crest:

(0) Absent

(1) Present

3. Mandible angular process – receiving structure for ectotympanic:

(0) Medially facing concavity for ectotympanic

(1) Posteriorly facing groove for ectotympanic

4. Meckel's groove to ventral margin of mandible:

(0) Convergent to the ventral margin

(1) Parallel to ventral margin

5. Replacement dental lamina (Crompton's) groove (visible along the lingual alveolar margin of last molars):
(0) Present
(1) Absent

Upper Molar Characteristics

6. Transversely widening of upper molars:
(0) Absent
(1) Present

7. Mesiolingual cusp X of upper molars: wear facets on the labial aspect of the cusp:
(0) Absent
(1) Wear facets present on the labial side of the lingual cusp

8. Transverse mesio-lingual and mesio-labial crests between Cusp A and Cusp X on anterior molars:
(0) Absent
(1) Present and complete

9. (New). Transverse mesio-lingual and mesio-labial crests between Cusp A and Cusp X on posterior molars:
(0) Absent
(1) Present and complete

10. Cusp Y (=upper disto-lingual cusp):
(0) Absent or indistinctive
(1) Present as a distinctive cusp
(2) Present, as crest aligned in antero-posterior line

11. Size and development of Cusp C (disto-labial cusp) and its separation from Cusp A (mesio-lingual cusp):
(0) Cusp C present and enlarged
(1) Reduced cusp C twinned with cusp A

12. Posterior transverse crest extending from the disto-labial (C) to the posterior cingulum (modified according to comment by Averianov et al., 2010):
(0) Absent

(1) Present

13. Presence of Cusp E separated from cusp B on posterior upper molars.
(0) Present
(1) Cusp E present and in labiolingual alignment with cusp B
(2) Absent

14. Constricted waist between the labial part and the lingual part of the upper tooth.
(0) Absent
(1) Present

Lower Molar Characteristics

15. Cusp c on lingual cingulid and in alignment with mesio-lingual cusp g (mesio-lingual):
(0) Absent
(1) Present

16. The a-c v-notch crest (postero-main crest of Sigogneau-Russell, 2003):
(0) Present
(1) Absent

17. Presence vs. absence and size of cusp g (mesio-lingual):
(0) Absent
(1) Small
(2) Distinctive, opposite to primary cusp a
(3) Distinctive, anteriorly positioned (more anteriorly placed than primary cusp a)
(4) Anteriorly placed and hypertrophied (to the same size as, or larger than cusp c)

18 Cusp c to cusp g size ratio:
(0) Cusp c much larger than cingular cusp g (if the latter is present)
(1) Sub-equal to the mesiolingual cusp g

19. Development of pseudo-talonid:
(0) Absent
(1) Present and its anterior-border by b-g crest

(2) Present and its anterior-border by b-e crest
(3) Present buy cusp b is much taller than g so the pseudotalonid appears to be lingually open

20. Raised a-g crest:
(0) Absent
(1) Present or lower
(2) Raised, with v-notch

21. Crest b-g:
(0) Absent, or weakly developed
(1) Present

22. The c-d crest in the posterior basin – presence/absence and alignment:
(0) Absent
(1) Present, c-d crest or c-f-d crests straight
(2) Present, c-d crest angled

23. Crest extending from cusp c to cusp df or the cusp df position:
(0) Absent
(1) Present

24. Placement of cusp d (modified from Sigogneau-Russell 2003: character 7; Luo & Martin 2007 Character 16; assuming homology of the morganucodontan cusp d to docodontan cusp d):
(0) Labial position (in alignment with a-b crest, or nearly so)
(1) Median placement (nearly halfway along the transverse width of posterior crown)

25. Distal Cusp d-f (=cusp dd of Hu et al. 2007):
(0) Absent
(1) Present

26. Folding enamel (on either upper or lower) (Sigogneau-Russell, 2003: character 5; Luo & Martin 2007 Character 17, scored on the posterior face of lower cusp a or lingual face of upper cusps A-C):
(0) Absent or weakly developed
(1) Present

27. Connecting structure of cusps a and d (modified from Luo and Martin

2007 character 19; Hu et al. 2007, Character 14):
(0) Not connected
(1) Incomplete
(2) Connected by a crest with a v-notch

28. Alignment of posterior crest of cusp a toward cusp d (postero-main crest of Sigogneau-Russell 2003; as defined in Luo & Martin 2007 character 18):
(0) Present and straight
(1) Present and angled

29. The b-g Crest - Crest between the mesio-labial cusp and mesio-lingual cusps:
(0) Absent
(1) Present, low and broken (v-valley)
(2) Present and continuous

30. Size of cusp e:
(0) Present and distinctive
(1) Reduced

31. Mesiolingual cingulid (width would be related with presence/absence of cusp e):
(0) Narrow or absent
(1) Wide

32. Mesio-lingual line-like cingulid extending from cuspule e or an equivalent position:
(0) Connected to cusp g
(1) Extending posteriorly to below the cusp g
(2) Absent or limited to the mesial part of the tooth

33. Size ratio of cusp b and cusp a:
(0) Large, well separated by a notch from cusp a
(1) Small, approximated to cusp a

34. Cusp b position:
(0) Close to cusp a
(1) Well-separated from cusp a by a deep notch

35. The “docodont cusp f” (Postero-lingually positioned as defined by Martin and Averianov 2004: figs 3 and 5, and differing from mesio-labially positioned cusp f; Luo & Martin 2007 character 24):
(0) Absent
(1) Present

36. The “standard cuspule f” (mesio-labially positioned, as defined by Kielan-Jaworowska et al. 2004: fig. 5.9: ‘mesiolabial cusp’. We follow Luo & Martin 2007 [character 25] in regarding this cusp to be different from cusp g in posterolingual position):
(0) Absent
(1) Present

37. The b-e crest:
(0) Absent
(1) Present and continuous from cusp b to the cingulid
(2) Present, as a part of the pseudotalonid rim

38. Anterior basin:
(0) No basin
(1) Small concavity
(2) Pseudotalonid basin

39. Distal basin:
(0) Absent
(1) Present

40. Width ratio of anterior basin vs. distal basin (modified from Hu et al. 2007 character 21, measured at the level of cusps/crests on occlusal surface):
(0) Posterior basin narrower than anterior basin (or anterior part of the tooth)
(1) Posterior basin wider than anterior basin

41. Interlock of lower molars:
(0) No interlock
(1) d-b-e interlock
(2) d – ‘standard-f’-e interlock
(3) d-“f”-e interlock
(4) d-b overlap

42. Placement of lower cusp E:
(0) Lingual position (lingual to the median axis of the lower molar)
(1) Cusp e labially shifted

43. Cusp triangulation (cusp triangulation between the a–c crest and the a–b crest following Butler 1997; Sigogneau–Russell and Godefroite 1997; Luo & Martin 2007 character 28):
(0) Absent
(1) Present

44. Degree of triangulation of cusps g–a–c:
(0) Broad triangle (>80 degrees)
(1) Sharp–triangled (≤80 degrees)

45. Gibbousness of crown base overhanging the roots at crown–root junction (scored at the middle molar[s] if multiple molars are known):
(0) Absent
(1) Present

46. Number of upper molariform roots:
(0) Two
(1) Three

47. Number of lower canine roots :
(0) One
(1) Two

Additional character in this analysis -
48. Presence of an anterior fovea on the upper molars:
(0) absent
(1) present and positioned at mid-line constriction of upper molar
(2) present and lingually offset from the midline of the upper molar

LITERATURE CITED

Averianov, A. O., A. V. Lopatin, S. A. Krasnolutskii, and S. V. Ivantsov. 2010. New docodontans from the Middle Jurassic of Siberia and reanalysis of Docodonta interrelationships. Proceedings of Zoological Institute of Russian Academy of Sciences 314:121–148.

Butler, P. M. 1997. An alternative hypothesis on the origin of docodont molar teeth. Journal of Vertebrate Paleontology 17:435-439.

Hu, Y.-M., J. Meng, J. M. Clark, A new Late Jurassic docodont (Mammalia) from northeastern Xinjiang, China. Vertebr. Palasiatica 45:173–194.

Kielan-Jaworowska, Z., R. L. Cifelli, and Z.-X. Luo. 2004. Mammals from the age of dinosaurs: origins evolution and structure. Columbia University Press, New York, N.Y., 630 pp.

Luo Z.-X., and T. Martin. 2007. Analysis of molar structure and phylogeny of docodont genera. Bulletin of the Carnegie Museum of Natural History 39:27–47.

Martin, T., and A. O. Averianov. 2004. A new docodont (Mammalia) from the Middle Jurassic of Kyrgyzstan, Central Asia. Journal of Vertebrate Palaeontology 30:855–871.

Martin, T., M. Nowotney, and M. Fischer. 2010. New data on tooth replacement in the Late Jurassic docodont mammal *Haldanodon exspectatus*. Society of Vertebrate Paleontology 70th Annual Meeting. Program and Abstracts:130A.

Meng, Q.-J., Q. Ji, Y. Zhang, D. Liu, D. M. Grossnickle, and Z.-X. Luo. 2015. An arboreal docodont from the Jurassic and mammaliaform ecological diversification. Science 347:760–764.

Pfretzschner, H. U., T. Martin, A. T. Matzke, and G. Sun. 2005. A new docodont mammal from the Late Jurassic of the Junggar Basin in Northwest China. Acta Palaeontologica Polonica 50:799–808.

Sigogneau-Russell, D. 2003. Docodonts from the British Mesozoic. Acta Palaeontologica Polonica 48:357–374.

Sigogneau-Russell, D., and P. Godefroit. 1997. A primitive docodont (Mammalia) from the Upper Triassic of France and the possible therian affinities of the order. Comptes-Rendus de l'Académie des Sciences, Paris, sér. IIa 324:135–140.